bioRxiv preprint doi: https://doi.org/10.1101/2022.11.06.515336; this version posted November 7, 2022. The copyright holder for this preprint (which was not certified by peer review) is the author/funder, who has granted bioRxiv a license to display the preprint in perpetuity. It is made available under aCC-BY 4.0 International license.

Title: Early-life language deprivation affects specific neural mechanisms of semantic representations

Authors: Xiaosha Wang[1,2*], Bijun Wang[1,2], Yanchao Bi[1,2,3*]

Affiliations: [1] State Key Laboratory of Cognitive Neuroscience and Learning & IDG/McGovern Institute for Brain Research, Beijing Normal University, Beijing, 100875, China. [2] Beijing Key Laboratory of Brain Imaging and Connectomics, Beijing Normal University, Beijing, 100875, China. [3] Chinese Institute for Brain Research, Beijing, China.

* Correspondence to X. Wang (email: wangxiaosha@bnu.edu.cn) and Y. Bi (email: ybi@bnu.edu.cn).

Abstract

One signature of the human brain is its ability to derive knowledge from language inputs, in addition to nonlinguistic sensory channels such as vision and touch. How does human language experience specifically modulate the way in which semantic knowledge is stored in the human brain? We investigated this question using a unique early-life language-deprivation human model: early deaf adults who are born to hearing parents and thus had delayed acquisition of any natural human language (speech or sign), with early deaf adults who acquired sign language from birth as nonlinguistic sensory experience controls. Neural responses in a meaning judgment task with 90 written words that were familiar to both groups were measured using fMRI. The early language-deprived group, compared with the deaf control group, showed reduced semantic sensitivity, in both multivariate pattern (semantic structure encoding) and univariate (abstractness effect) analyses, in the left dorsal anterior temporal lobe (dATL). These results provide positive, causal evidence that the neural semantic representation in dATL is specifically supported by language, as a unique mechanism of representing (abstract) semantic space, beyond the sensory-derived semantic representations distributed in the other cortical regions.

Keywords: dorsal anterior temporal lobe; fMRI; knowledge; language; semantics

bioRxiv preprint doi: https://doi.org/10.1101/2022.11.06.515336; this version posted November 7, 2022. The copyright holder for this preprint (which was not certified by peer review) is the author/funder, who has granted bioRxiv a license to display the preprint in perpetuity. It is made available under aCC-BY 4.0 International license.

Introduction

Humans are believed to be the only species in the animal kingdom where knowledge learning can be achieved symbolically, mostly through language ("roses are red"), in addition to sensory channels (visually perceiving roses in color red) (Gelman and Roberts, 2017; Perszyk and Waxman, 2018). A common view shared by the modern neurocognitive theories of semantics is that semantic knowledge, even those acquired through language, is ultimately grounded in (nonlinguistic) sensory/motor experiences, encoded in the distributed brain areas encompassing high-level sensorimotor areas, and potential hub regions that bind such sensory-derived representations (Barsalou, 2016; Binder et al., 2009; Fernandino et al., 2022; Lambon Ralph et al., 2017; Martin, 2016). Are there neural structures that specialize to represent knowledge derived from language experience, and not (nonlinguistic) sensory experience?

Neural representations of fully nonsensory, language-derived knowledge have only recently been inferred based on studies with sensory-deprived individuals (Bottini et al., 2020; Striem-Amit et al., 2018; Wang et al., 2020, see (Bi, 2021) for a review). Congenitally blind individuals, who cannot acquire visual-specific knowledge (e.g., color) through sensory experiences, can nevertheless acquire semantic structures about such knowledge behaviorally similar to those in the sighted, presumably derived from language. Such nonsensory semantic structures in the blind (and also sighted) are represented in the dorsal anterior temporal lobe (dATL), with sighted individuals additionally representing the highly similar knowledge structure (presumably derived from sensory experience) in the visual cortex (Wang et al., 2020). This dATL cluster is distinct from the central "amodal" semantic hub proposed to bind together multiple sensory attributes, which lies in the more ventral-medial territory of the ATL (Lambon Ralph et al., 2017; Patterson et al., 2007; see discussions in Striem-Amit et al., 2018). The left dATL is also more strongly activated by abstract

bioRxiv preprint doi: https://doi.org/10.1101/2022.11.06.515336; this version posted November 7, 2022. The copyright holder for this preprint (which was not certified by peer review) is the author/funder, who has granted bioRxiv a license to display the preprint in perpetuity. It is made available under aCC-BY 4.0 International license.

than concrete words in typically developed individuals (Binder et al., 2009; Bucur and Papagno, 2021; Wang et al., 2010, 2019), corroborating the role of this area in representing knowledge derived from language (see discussions in Bi, 2021). These lines of evidence, while highly suggestive, are based on manipulating sensory experience by examining individuals deprived of a sensory modality or by contrasting concepts with rich sensory experiences versus those without, rather than the positive manipulation of language experience. Thus the positive evidence for the necessity of language experiences for the neural semantic representation here is still lacking.

Here, we take advantage of a special early-life language-deprivation human model: individuals who were born profoundly deaf in hearing families and thus had very limited natural language exposure (speech or sign) during the critical period of language acquisition in early childhood (Goldin-Meadow and Feldman, 1977; Mayberry et al., 2002). These individuals usually acquired their first language (sign language) around school age, which is much later than the age of first language (L1) acquisition in typically developed children or native deaf signers who were born in deaf families and acquired sign language from birth. Previous research has shown that these delayed deaf signers have lower proficiency in phonological, morphological, and syntactic processing of sign language (Bogliotti et al., 2020; Caselli et al., 2021; Cheng and Mayberry, 2021; Lieberman et al., 2015; Mayberry et al., 2002; Mayberry and Fischer, 1989; Newport, 1990; Tomaszewski et al., 2022) and decreased neural activation in language areas (Mayberry et al., 2018, 2011; Richardson et al., 2020; Twomey et al., 2020) even after many years of sign language usage, indicating long-lasting hypofunction of the language system as a result of missing the critical period of language acquisition. The effects of early language deprivation on semantic processing have been scarcely studied and the extant pieces of evidence reported minimal influences in semantics-related behavioral or N400 measures in adult signers (Baus et al., 2008; Davidson and Mayberry, 2015;

bioRxiv preprint doi: https://doi.org/10.1101/2022.11.06.515336; this version posted November 7, 2022. The copyright holder for this preprint (which was not certified by peer review) is the author/funder, who has granted bioRxiv a license to display the preprint in perpetuity. It is made available under aCC-BY 4.0 International license.

77 Skotara et al., 2012). Given that semantic processing is supported by a multifaceted cognitive
78 system and a complex neural network entailing distributed semantic regions (Bi, 2021; Binder and
79 Desai, 2011; Lambon Ralph et al., 2017; Martin, 2016), the comparable behavioral performances do
80 not indicate comparable neural structures (e.g., color knowledge in the blind and sighted people
81 (Wang et al., 2020)). We compared native and delayed deaf signers in terms of their fMRI BOLD
82 responses to meaning judgment to examine their neural substrates of semantic processing of words
83 that are familiar to them. That is, by a rare opportunity of manipulation of early language
84 experience offered by nature, we empirically examined the specific role of language experience in
85 the semantic neural representation.
86
87 **Results**
88
89 ***Participants' background information and task fMRI design***
90 We recruited two adult groups of congenitally or early deaf participants (Table 1), including 16 with
91 native sign language acquisition (native deaf signers) and 23 with delayed language acquisition
92 (delayed deaf signers). Native signers were born in deaf families; delayed signers were born in
93 hearing families and became exposed to Chinese sign language (CSL) between the ages of 4 and 10
94 (mean ± standard deviation (SD): 6.91 ± 1.62 years old). The family signing environment was
95 confirmed by the subjective ratings of parental CSL proficiency: Native signers rated their parents to
96 have much more proficient CSL skills than delayed signers did on a 7-point scale (Welch's $t_{31.7}$ =
97 13.54, $p = 1.10 \times 10^{-14}$; each participant provided CSL ratings for both parents and the maximum
98 score was used for group comparison). All deaf participants received formal education in special
99 education programs since elementary school. The two deaf groups were matched on demographic
100 variables (gender, age, years of education, *p*s > .15) and subjective social status (Adler et al., 2000)

bioRxiv preprint doi: https://doi.org/10.1101/2022.11.06.515336; this version posted November 7, 2022. The copyright holder for this preprint (which was not certified by peer review) is the author/funder, who has granted bioRxiv a license to display the preprint in perpetuity. It is made available under aCC-BY 4.0 International license.

during childhood (p = .54). While the two groups significantly differed in the education levels of their parents (Table 1; ps < .053), the direction was in favor of delayed signers as their hearing parents received more formal education than the deaf parents of native signers. In terms of language skills, the two deaf groups were matched on self-reported proficiency of CSL comprehension, production, and lipreading skills (ps > .34), and on the reading disability risk measured by the adult reading history questionnaire (Lefly and Pennington, 2000) (p = .22). Written word processing was further evaluated in two reaction-time tasks (i.e., visual lexical decision and word-triplet semantic judgment) and no significant group differences were found (Supplementary file 1). In summary, the native and delayed deaf groups were carefully matched on a wide range of demographic and later language performances (sign, lipreading, and written). Thus the early language deprivation is a strong candidate to account for the neural group differences reported below.

The stimuli of task fMRI were 90 written words that were highly familiar to both groups, including 40 concrete/object words varying in sensory and motor properties (animals, face/body parts, artefacts) and 50 abstract/nonobject words varying in social and emotional contents. These words could be grouped into 10 categories based on the group-averaged semantic multi-arrangement performances in an independent group of 32 hearing participants (see Methods, Figure 1a, and Figure 1-figure supplement 1). Both deaf groups judged these words to be highly familiar (7-point familiarity ratings from 8 native signers: 6.72 ± 0.17; 13 delayed signers: 6.86 ± 0.15; 7 being most familiar) and yielded similar word-relational structures in a 1-hour semantic distance judgment task, in which each participant (16 native and 21 delayed signers) produced a 90 × 90 semantic distance matrix (RDM). The group-averaged semantic RDMs of the two deaf groups were strongly correlated (Spearman rho = 0.71, n = 4005; Figure 1a). At the individual level, correlations with the benchmark

bioRxiv preprint doi: https://doi.org/10.1101/2022.11.06.515336; this version posted November 7, 2022. The copyright holder for this preprint (which was not certified by peer review) is the author/funder, who has granted bioRxiv a license to display the preprint in perpetuity. It is made available under aCC-BY 4.0 International license.

(the group-averaged RDM of hearing participants) did not significantly differ between the two deaf groups (Welch's $t_{31.30}$ = -0.37, p = .71).

In the MRI scanner, participants were asked to think about the meaning of each of the 90 words (condition-rich fMRI design (Kriegeskorte et al., 2008a)) and to decide whether a word in red (catch trials) was semantically related to its previous word (i.e., oddball one-back semantic judgment, Figure 1b). We first examined the two-deaf-group differences in brain regions preferring abstract/nonobject words to concrete/object words, which have been proposed to relate to verbal semantic processing (Binder et al., 2009; Wang et al., 2010). These regions were functionally localized by contrasting abstract/nonobject words (e.g., *reason*) to concrete/object words (e.g., *panda*) in an independent group of 33 hearing participants (voxel-level $p < .001$, cluster-level FWE-corrected $p < .05$). This contrast in the hearing group resulted in regions in the frontal and temporal cortices that were well aligned with the literature (Figure 1c and Figure 1-figure supplement 2). In particular, the left dATL, the left inferior frontal gyrus (IFG), and the left posterior middle temporal region (pMTG) were most consistently reported in the meta-analyses (Binder et al., 2009; Bucur and Papagno, 2021; Wang et al., 2010) and were taken as our primary regions of interest (ROIs). Results for the other clusters are shown in Figure 1-figure supplement 3 (no significant group differences). We then carried out whole-brain analyses to explore the two-deaf-group differences beyond these semantic ROIs. We focused on two neural semantic effects: 1) multivoxel pattern representation of word meaning (i.e., semantically related words have similar neural patterns); and 2) the univariate semantic abstractness effects. It should be noted that the neural semantic abstractness effect does not equate with language-derived semantic knowledge, as it might arise from some nonverbal cognitive processes that are more engaged in abstract word processing (Binder et al., 2016). The reasoning here is that if a brain region's

bioRxiv preprint doi: https://doi.org/10.1101/2022.11.06.515336; this version posted November 7, 2022. The copyright holder for this preprint (which was not certified by peer review) is the author/funder, who has granted bioRxiv a license to display the preprint in perpetuity. It is made available under aCC-BY 4.0 International license.

abstractness effect is affected by early language deprivation, this would constitute further evidence that the abstractness computed by this brain region is indeed associated with language processes.

Semantic structure representation: dATL alteration in delayed signers

We first examined whether early-life language deprivation affects neural representations of the semantic space using representational similarity analysis (RSA, Figure 2a) (Kriegeskorte et al., 2008a, 2008b). We estimated the multivoxel activation pattern for each target word and, in a given ROI, calculated the correlation distance (1-Pearson correlation) of the multivoxel activation patterns between each word pair to build a 90 x 90 neural representational dissimilarity matrix (RDM). As a sanity check, we first carried out whole-brain searchlight RSA of visual similarity of written words, by computing Spearman's rank correlation between the pixelwise dissimilarity of the 90 words and neural RDMs, and observed significant encoding of written word visual similarity in the early visual cortex in both native and delayed signers at the threshold of voxel-level $p < .001$, cluster-level FWE-corrected $p < .05$ (Supplementary file 2). To quantify the semantic information encoded in the neural RDMs, we computed Spearman's partial correlation between the neural RDMs and the 10-category benchmark semantic RDM (i.e., those of the hearing group), while controlling for the stimulus low-level visual and phonological RDMs.

ROI-level RSA was carried out in the left dATL, pMTG, and IFG. As shown in Figure 2b, the three ROIs significantly encoded the semantic space in native signers ($t_{15} > 3.04$, one-tailed ps $< .004$, Cohen's $d > 0.76$). In delayed signers, the left dATL and pMTG significantly encoded semantic space ($t_{22} > 2.07$, one-tailed ps $< .025$, Cohen's $d > 0.43$) and the left IFG showed a similar, nonsignificant, trend ($t_{22} = 1.31$, one-tailed $p = 0.10$, Cohen's $d = 0.27$). Critically, group differences were observed in the left dATL (Welch's $t_{36.7} = 3.15$, two-tailed $p = .003$, Hedges' $g = 0.98$), not in the left pMTG or IFG

bioRxiv preprint doi: https://doi.org/10.1101/2022.11.06.515336; this version posted November 7, 2022. The copyright holder for this preprint (which was not certified by peer review) is the author/funder, who has granted bioRxiv a license to display the preprint in perpetuity. It is made available under aCC-BY 4.0 International license.

(*p*s > .26). For the left dATL, we further computed a partial correlation between neural RDMs and the semantic RDM, controlling for the object-vs-nonobject category structure. The reduction in the delayed group compared with native signers still held (Welch's $t_{30.4}$ = 2.91, two-tailed p = .007, Hedges' g = 0.93), indicating that language-deprivation-induced semantic-encoding downregulation was beyond the object-vs-nonobject binary distinction in the left dATL.

We then carried out whole-brain searchlight RSA (Kriegeskorte et al., 2006) to explore group differences in semantic encoding beyond the semantic ROIs defined above (Figure 2c and Figure 2-figure supplement 1). At the threshold of voxel-level p < .001, cluster-level FWE-corrected p < .05, in native signers, the semantic encoding was observed in the left dATL, IFG, pMTG, along with adjacent parietal and occipital areas, dorsomedial prefrontal cortex, and frontal orbital cortex. In delayed signers, no brain regions survived the whole-brain correction; at a more lenient threshold of voxel p < .001, cluster size > 10 voxels, semantic encoding could be observed in the left dATL, IFG, and clusters scattered in the left inferior parietal and occipital regions. Importantly, the whole-brain contrast between the two deaf groups peaked at the left dATL at the threshold of voxel p < .001, which was also the largest cluster (Brodmann area 21/38, peak MNI coordinates: -60, 6, -20, peak t = 5.87, 162 voxels), converging well with the ROI results in that native signers showed stronger semantic encoding than delayed signers in the left dATL ROI. While this cluster was not large enough to survive the whole-brain correction (cluster FWE-corrected p = .22), the top 10 voxels survived the voxel-level correction of FWE-corrected p < .05. No areas were found to show significantly increased semantic information in delayed signers compared with native signers at the conventional threshold.

bioRxiv preprint doi: https://doi.org/10.1101/2022.11.06.515336; this version posted November 7, 2022. The copyright holder for this preprint (which was not certified by peer review) is the author/funder, who has granted bioRxiv a license to display the preprint in perpetuity. It is made available under aCC-BY 4.0 International license.

Univariate semantic abstractness effects: dATL alteration in delayed signers

We then examined how early language deprivation might alter the neural semantic abstractness effects by comparing regional activation strength to abstract/nonobject and concrete/object words in two deaf groups. At the ROI level, all three ROIs (the left dATL, IFG, and pMTG) exhibited significant abstractness preference in both deaf groups (Figure 3a; native group: paired *t*s > 3.72, df = 15, one-tailed *p*s < .001, Cohen's *d*s > 0.93; delayed group: paired *t*s > 2.13, df = 22, one-tailed *p*s < .02, Cohen's *d*s > 0.44), further indicating the robustness of semantic abstractness preference in these ROIs. We then carried out two-way ANOVA to examine group effects in each of these ROIs, with word type (concrete/object, abstract/nonobject) as a within-subject factor and group (native, delayed) as a between-subject factor. The group × word-type interaction reached statistical significance in only the left dATL ($F_{(1,37)}$ = 4.91, p = .033), not in the left pMTG or IFG (*p*s > .30). In the left dATL native signers exhibited greater semantic abstractness effects than delayed signers. The main effects of group were not significant in any of the three ROIs (*p*s > .057).

Considering inter-subject variations in activation locations, we further carried out the individualized functional region-of-interest (fROI) analysis for validation (Cohen et al., 2019; Murty et al., 2020) (see Methods). Using each of the ROIs defined in the hearing group as anatomical constraints, we identified the top 50 selective voxels in each deaf participant using one-half of the fMRI data and computed regional activation strength to abstract and concrete words in these voxels in the held-out data (i.e., via an odd-even run cross-validation process). As shown in Figure 3b, the group × word-type interaction was again observed in the left dATL ($F_{(1,37)}$ = 6.20, p = .017), not in pMTG or IFG (*p*s > .58); main effects of group were not found (*p*s > .18).

We further carried out a whole-brain analysis of the semantic abstractness effects in the two deaf

bioRxiv preprint doi: https://doi.org/10.1101/2022.11.06.515336; this version posted November 7, 2022. The copyright holder for this preprint (which was not certified by peer review) is the author/funder, who has granted bioRxiv a license to display the preprint in perpetuity. It is made available under aCC-BY 4.0 International license.

groups (Figure 3-figure supplement 1). At the threshold of voxel-level $p < .001$, cluster-level FWE-corrected $p < .05$, semantic abstractness reached significance in the left dATL in native signers (Brodmann area 21/38/22, peak MNI coordinates: -58, 4, -8, peak t = 7.27, 209 voxels). No regions survived the whole-brain threshold in delayed signers; at a lenient threshold of voxel $p < .001$, cluster size > 10 voxels, abstractness can be observed in the left pMTG and dATL, which are consistent with the ROI results above. For the whole-brain comparisons of the semantic abstractness effects between the two deaf groups, no areas survived the conventional threshold; small scattered clusters (cluster sizes < 14 voxels) were observed at a lenient threshold of voxel $p < .001$.

Discussion

By comparing fMRI BOLD responses to the word semantic structures between native and delayed early deaf signers, we aimed to examine how the critical-period, early-life language experience affects the semantic neural representations. Our results demonstrated that semantic information in the left dATL was significantly reduced in delayed signers compared with native signers in both multivariate (representation of rich semantic space) and univariate (preference to abstract/nonobject words) analyses. That is, early-life language acquisition—critical to language system neurodevelopment—is necessary for the left dATL to exhibit the typical semantic organization in adulthood. Such evidence provides the first positive evidence for the effect of language experience in driving the semantic functional development of a particular brain region.

First, what kind of variables best account for the current group contrast results? The two deaf

bioRxiv preprint doi: https://doi.org/10.1101/2022.11.06.515336; this version posted November 7, 2022. The copyright holder for this preprint (which was not certified by peer review) is the author/funder, who has granted bioRxiv a license to display the preprint in perpetuity. It is made available under aCC-BY 4.0 International license.

groups were matched on sensory-experiences (both similarly profound deaf), a wide range of nonlinguistic environmental variables including the socioeconomic status (except for parents' education backgrounds, which were better for the delayed signer group), the length and level of formal education, through which largely comparable sign language and word reading skills were achieved. The salient difference was the early-life language experience (before 6.9 years old -- the mean age of acquisition in our delayed signer group). Notably, deaf children with early language deprivation often spontaneously develop homesign systems, which share some aspects with natural language (Goldin-Meadow, 2003). For instance, they could use homesigns to produce generic utterances, more so for animals than for artefacts (Goldin-Meadow et al., 2005). Critically, our positive results of the robust group differences in dATL suggest that early homesign and later formal education for sign and written language experiences are insufficient for typical dATL neurodevelopment; the full-fledged language experience during the critical period (before school age) plays a necessary role in this process. A further variable to consider is that early language deprivation may lead to alterations beyond the language system, affecting non-language cognitive domains such as working memory or theory of mind in children (Marshall et al., 2015; Richardson et al., 2020). While we cannot rule out the effects of these potential intermediate cognitive processes, the positive evidence of these variables in dATL functionality is lacking. The most direct manipulation and parsimonious account for the dATL effects is language related (see below).

Importantly, the specific effects of language experience in shaping the semantic representation in dATL observed here are corroborated by several previous lines of indirect evidence for the relevance of language in its functionality. It shows a functional preference for abstract words, which are less salient in sensory attributes than concrete words, and are assumed to entail more language processes such as context diversity (e.g., Binder et al., 2009; Bucur and Papagno, 2021; Wang et al.,

bioRxiv preprint doi: https://doi.org/10.1101/2022.11.06.515336; this version posted November 7, 2022. The copyright holder for this preprint (which was not certified by peer review) is the author/funder, who has granted bioRxiv a license to display the preprint in perpetuity. It is made available under aCC-BY 4.0 International license.

2010). In congenitally blind individuals, it encodes visual knowledge such as color and is negatively modulated by perceptibility (Bottini et al., 2020; Striem-Amit et al., 2018; Wang et al., 2020). It was further shown recently that left ATL encodes specific higher-order statistical relations (i.e., graph) among words computed from word co-occurrences patterns within the language system (Fu et al., 2022). It has also been shown to be sensitive to semantic composition, such as in two-word phrases or sentences (Pallier et al., 2011; Pylkkänen, 2019). This region is functionally and structurally connected with other language-sensitive regions (Fan et al., 2014; Friederici et al., 2017; Lambon Ralph et al., 2017; Pascual et al., 2015; Wang et al., 2019). Finally, neurodevelopmental evidence also highlighted the importance of dATL in early language and semantic development. A recent study (Yu et al., 2021) showed that the resting-state functional connectivity patterns of the middle portion of the left temporal pole in infancy and toddlerhood significantly predict performances in tasks entailing semantic processes (i.e., the Picture Vocabulary and Oral Comprehension tests), not in tasks of phonological skills or rapid automatized naming, at about 6.5 years old; this prospective association is modulated by early language skills, as controlling for early language skills significantly reduces the association. This compelling neurodevelopmental pattern indicates the dATL-related network as a neural scaffold for subsequent accumulation of language-related semantic knowledge. These lines of findings are often correlational evidence for the language effect on their own. Together with the positive evidence of early language experience in developing typical semantic representation in dATL reported here, the parsimonious proposal accounting for them together would be that dATL represents knowledge derived from language (e.g., from higher-order word relations), and that nonsensory, abstract meanings are more strongly supported by such language information. With critical period language deprivation, the semantic structure representation and the abstract preference here are reduced.

bioRxiv preprint doi: https://doi.org/10.1101/2022.11.06.515336; this version posted November 7, 2022. The copyright holder for this preprint (which was not certified by peer review) is the author/funder, who has granted bioRxiv a license to display the preprint in perpetuity. It is made available under aCC-BY 4.0 International license.

Interestingly, the semantic effects did not significantly differ between the two deaf groups in the left IFG and pMTG, two other brain regions widely implicated in language and semantic processing, also with an abstractness preference (Binder et al., 2009; Friederici et al., 2017; Lambon Ralph et al., 2017; Wei et al., 2012; Xu et al., 2017). In the early-language deprivation model, previous studies found that delayed signers show reduced activity in posterior temporal regions and/or IFG in multiple sign language sentence judgment tasks (Mayberry et al., 2011; Twomey et al., 2020) and increased IFG activity in phonological judgment (MacSweeney et al., 2008). Reduced fractional anisotropy (FA) values in the left dorsal arcuate fasciculus structurally connecting the two regions have been reported in three cases with post-childhood first-language acquisition (Cheng et al., 2019). These results indicate that the development of the dorsal language pathway, particularly those substrates supporting the syntactic and/or phonological processes, is indeed shaped by early language experience. Our results show that the semantic processes in these regions were not affected by the changes in nonsemantic language functions (e.g., phonology). While the detailed functional relations among these regions and dATL are unclear, the relatively salient role of ATL in language-supported semantics is consistent with the dynamic causal modeling results that identified the ATL (not IFG, MTG, or inferior parietal areas) as the early hub (within 250 ms) for abstractness effects, followed by inferior parietal areas as a late hub, across three electro/magnetoencephalography tasks (Farahibozorg et al., 2022). Therefore, while other brain regions may also contribute to language-supported semantics, a detailed neuroanatomical framework is needed to accommodate why language-related semantic effects peak in the dATL.

What are the implications of the current findings for neurocognitive models of semantics and semantic behaviors? The relationship between the current neural results and semantic behaviors is intriguing. On the one hand, these findings about how language experience is critical for specific

bioRxiv preprint doi: https://doi.org/10.1101/2022.11.06.515336; this version posted November 7, 2022. The copyright holder for this preprint (which was not certified by peer review) is the author/funder, who has granted bioRxiv a license to display the preprint in perpetuity. It is made available under aCC-BY 4.0 International license.

316 semantic neural structures (dATL) are in line with the rich evidence and discussion in the behavioral
317 literature about the role of language in semantic development. For instance, developmental
318 behavioral evidence shows that young human infants are sensitive to language labels and statistical
319 patterns in forming semantic categories and other types of semantic relations (Perszyk and Waxman,
320 2018; Unger and Fisher, 2021; Spelke, 2017; see similar discussions in Gelman and Roberts, 2017;
321 Lupyan et al., 2020). On the other hand, consistent with previous behavioral studies of semantic
322 processing in delayed adult signers (Baus et al., 2008; Davidson and Mayberry, 2015; Skotara et al.,
323 2012), in our study native and delayed signers exhibited similar semantic space for words that they
324 are familiar with (Figure 1a) and did not significantly differ in two additional reaction time tasks
325 (Supplementary file 1). That is, we did not see visible semantic behavioral differences despite the
326 reduced dATL semantic representation. This seeming conflict is likely related to the multifaceted
327 nature of the cognitive and neural basis of semantics more broadly. Semantic processing entails
328 representations that can be derived from multiple types of experiences, supported by highly
329 distributed neural systems (e.g., Binder et al., 2009). In fact, many neurocognitive semantic theories
330 mainly focus on the representing, binding, and controlling of those knowledge derived from
331 nonlinguistic multisensory experiences, and are less committed about the kind of language-derived
332 neural semantic representations (Binder, 2016; Lambon Ralph et al., 2017; Martin, 2016; but see
333 Mahon and Caramazza, 2008). The two deaf groups are not assumed to differ in these nonlinguistic
334 aspects of semantic processing. The delayed signers may thus rely on these systems to achieve
335 comparable performances in the semantic tasks being tested. Our current findings that positively
336 show the specific effect of language experience on dATL and not on other regions are thus best
337 accommodated by a recently developed dual-neural-coding framework for semantic knowledge (Bi,
338 2021), which explicitly proposes that the human brain has developed specialized brain regions (the
339 dATL) for language-derived semantic representations, in addition to the sensory-derived knowledge

bioRxiv preprint doi: https://doi.org/10.1101/2022.11.06.515336; this version posted November 7, 2022. The copyright holder for this preprint (which was not certified by peer review) is the author/funder, who has granted bioRxiv a license to display the preprint in perpetuity. It is made available under aCC-BY 4.0 International license.

representations. Now with stronger evidence for the language-driven representation, future studies are warranted to examine the exact computational principles in the left dATL (e.g., Fu et al., 2022) and semantic behaviors more targeted at the functionality of this area than the general semantic tasks currently employed.

To conclude, by manipulation of early language experience by nature we were able to positively identify a human brain region – dorsal anterior temporal lobe -- specifically supporting word meanings derived from language experience, in contrast to those grounding nonlinguistic, sensory experiences. These findings highlight the unique role of language in forming specific neural semantic representations in the human brain, and raise new questions about the ontogenetic mechanisms of this intriguing neural structure.

Materials and Methods

Participants

Thirty-nine congenitally or early deaf adults and 33 hearing college students (15 males, mean age 21.97 ± 2.58 years, range: 18-28 years, all native Mandarin Chinese speakers) were recruited for the fMRI study. All except for 1 delayed deaf signer and 1 hearing participant participated in the behavioral semantic distance judgment task. The behavioral data of one delayed signer were excluded from data analysis due to technical errors. The behavioral and neural data of 21 out of the 33 hearing college students overlapped with a previous study (Wang and Bi, 2021) that examined the intersubject variability of semantics in typically developed populations.

Deaf participants included two groups (Table 1). Native signers (*n* = 16; 11 males) had deaf parents and were exposed to CSL soon after birth. Delayed (nonnative) signers (*n* = 23; 12 males) were born

bioRxiv preprint doi: https://doi.org/10.1101/2022.11.06.515336; this version posted November 7, 2022. The copyright holder for this preprint (which was not certified by peer review) is the author/funder, who has granted bioRxiv a license to display the preprint in perpetuity. It is made available under aCC-BY 4.0 International license.

364 in hearing families and learned CSL after they were enrolled in special education schools (range:
365 4-10 years old). All deaf participants completed a background questionnaire, in which they reported
366 their hearing loss conditions, history of language acquisition, and educational background. They
367 were also asked to rate sign language abilities of their family members and to rate their own sign
368 and lipreading abilities using a 7-point scale: 1 = none at all, 7 = very proficient. All deaf participants
369 then finished the Chinese version of the Adult Reading History Questionnaire (a self-report
370 screening tool for the risk of reading disability in adults (Lefly and Pennington, 2000)), the
371 MacArthur Scale of subjective social status (Adler et al., 2000) during childhood, and reported the
372 educational years of their parents. For hearing loss conditions, all deaf participants reported being
373 severely or profoundly deaf from birth, except for 1 native signer and 3 delayed signers who
374 reported becoming deaf before the age of 2 due to medication side effects. Hearing thresholds in
375 decibels (dB) were available in 23 deaf participants (native: 11/16; delayed: 12/23) and confirmed
376 severe to profound hearing loss (range: 85-120 dB). One native signer and 4 delayed signers were
377 using hearing aids at the time of testing; others either had never used hearing aids (6 native signers
378 and 5 delayed signers) or had used hearing aids for some time (9 native signers and 14 delayed
379 signers; years of use: 0.5-20 years). Speech comprehension was reported to be very poor, even with
380 the use of hearing aids.
381
382 All participants had normal or corrected-to-normal vision. All participants were right-handed,
383 except for three native signers (1 was ambidextrous and 2 were left-handed) (measured by the
384 Edinburgh inventory (Oldfield, 1971)). All participants gave written informed consent and received
385 monetary compensation for participation. The study was approved by the Human Subject Review
386 Committee at Peking University (2017-09-01), China, in accordance with the Declaration of Helsinki.
387

bioRxiv preprint doi: https://doi.org/10.1101/2022.11.06.515336; this version posted November 7, 2022. The copyright holder for this preprint (which was not certified by peer review) is the author/funder, who has granted bioRxiv a license to display the preprint in perpetuity. It is made available under aCC-BY 4.0 International license.

388 ***Word stimuli in task fMRI***

389 The stimuli for fMRI scanning were 90 written words, including 40 concrete/object words and 50
390 abstract/nonobject words without explicit external referents. Concrete/object words varied in
391 sensory and motor attributes and included 10 animals (e.g., *panda*), 10 face or body parts (e.g.,
392 *shoulder*), 10 tools (e.g., *hammer*), and 10 common large household objects (e.g., *microwave*).
393 Abstract/nonobject words varied in social and emotional associations (e.g., *cause*, *violence*). A
394 7-point familiarity rating, with 7 being the most familiar, was collected from 21 out of 39 deaf
395 signers and an independent group of 26 hearing college students. All words were highly familiar to
396 deaf participants (8 native signers: 6.72 ± 0.17; 13 delayed signers: 6.86 ± 0.15). All words were
397 disyllabic except for five object words ("cat" and "bed" are monosyllabic and "giraffe", "microwave",
398 and "washing machine" are trisyllabic in Chinese). All words were primarily used as nouns except for
399 10 words denoting emotional states (nine were primarily used as adjectives and one as a verb). The
400 concrete and abstract words were matched on the number of strokes (a measure of visual
401 complexity for Chinese words; 17.23 ± 5.80 vs. 16.14 ± 3.98; two-samples t_{88} = 1.05, p = .30). While
402 concrete/object words were less frequent in a Mandarin Chinese corpus (Sun et al., 1997) than
403 abstract/nonobject words (log word frequency: 1.05 ± 0.73 vs. 1.62 ± 0.68; t_{88} = -3.83, p < .001), the
404 former were rated as more subjectively familiar than the latter in either hearing (6.79 ± 0.16 vs.
405 6.22 ± 0.26; t_{88} = 12.05, p < .001) or deaf (6.85 ± 0.07 vs. 6.77 ± 0.13; t_{88} = 3.41, p < .001)
406 participants.

407

408 ***Behavioral semantic distance judgment task***

409 To examine participants' understanding of the 90 words used in the task fMRI, we asked them to
410 judge semantic distance among these words by arranging them spatially close together or far apart
411 in a circular arena on a computer screen via mouse drag-and-drop operations (Kriegeskorte and Mur,

bioRxiv preprint doi: https://doi.org/10.1101/2022.11.06.515336; this version posted November 7, 2022. The copyright holder for this preprint (which was not certified by peer review) is the author/funder, who has granted bioRxiv a license to display the preprint in perpetuity. It is made available under aCC-BY 4.0 International license.

2012). The task lasted for one hour and produced a 90 x 90 semantic distance matrix (i.e., a behavioral representational dissimilarity matrix, RDM) for each participant. Taking the hearing group-averaged semantic RDM as a benchmark, we correlated each deaf participant's semantic RDM with it using Spearman's rank correlation, Fisher-z-transformed the correlation coefficients, and compared the two deaf groups to assess the similarity between their semantic structures.

Considering the multidimensional and flexible nature of semantic distance among various concrete and abstract words (Binder et al., 2016; Conca et al., 2021), we focused on the categorical structure of 90 words that captured the large-scale semantic relationships and was likely to be shared across individuals. The categorical RDM was obtained by performing a k-means clustering analysis on the group-averaged 90 × 90 semantic RDM of hearing participants (the factoextra package, http://www.sthda.com/english/rpkgs/factoextra, in the R programming environment; Version 4.0.0; R Core Team, 2020). The optimal number of clusters was determined based on gap statistic (Tibshirani et al., 2001), which revealed 10 semantic categories (Figure 1a and Figure 1-figure supplement 1).

Task fMRI procedure

In the fMRI scanner, participants were instructed to look at each of the 90 target words, think about their meanings, and perform an oddball one-back semantic judgment task. In this oddball task, participants were asked to judge whether occasional words in red (catch trials) were semantically related to the previous word by pressing the corresponding buttons with the right index or middle finger.

Each participant performed 10 runs (360 s per run) of task fMRI scanning, except for one native

bioRxiv preprint doi: https://doi.org/10.1101/2022.11.06.515336; this version posted November 7, 2022. The copyright holder for this preprint (which was not certified by peer review) is the author/funder, who has granted bioRxiv a license to display the preprint in perpetuity. It is made available under aCC-BY 4.0 International license.

signer who finished eight runs and withdrew due to discomfort. Each run consisted of 90 2.5 s-long target word trials and 14 2.5 s-long catch trials. Each trial started with a 0.8-s word stimulus (black color, Song font, and 2.6 visual degrees in height) at the center of a gray background, followed by 1.7-s fixation. Thirty 2.5 s-long null trials (fixation only) were randomly inserted among target and catch trials, with the interval between two words ranging from 1.7 to 11.7 s. Each target word appeared once in each run, and the order was pseudorandomized for each run in each participant. Each run began with a 12-s fixation period and ended with a 13-s rest period during which participants received a written cue that the current run was about to end. Stimulus presentation was controlled by E-prime 2. The 140 catch trials were created by first pairing each of the 90 target words with a probe word and then pseudo-randomly selecting 50 out of 90 target words (21 concrete/object words and 29 abstract/nonobject words) to pair with another 50 probe words. Participants performed this task attentively, with overall miss rates lower than 22.1% (median: 1.4%).

Image acquisition

All functional and structural MRI data were collected using a Siemens Prisma 3T Scanner with a 64-channel head-neck coil at the Center for MRI Research, Peking University. Functional data were acquired with a simultaneous multi-slice echoplanar imaging sequence supplied by Siemens (62 axial slices, repetition time (TR) = 2000 ms, echo time (TE) = 30 ms, multi-band factor = 2, flip angle (FA) = 90°, field of view (FOV) = 224 mm × 224 mm, matrix size = 112 × 112, slice thickness = 2 mm, gap = 0.2 mm, and voxel size = 2 × 2 × 2.2 mm). A high-resolution 3D T1-weighted anatomical scan was acquired using the magnetization-prepared rapid acquisition gradient echo sequence (192 sagittal slices, TR = 2530 ms, TE = 2.98 ms, inversion time = 1100 ms, FA = 7°, FOV = 224 mm × 256 mm, matrix size = 224 × 256, interpolated to 448 × 512, slice thickness = 1 mm, and voxel size = 0.5

bioRxiv preprint doi: https://doi.org/10.1101/2022.11.06.515336; this version posted November 7, 2022. The copyright holder for this preprint (which was not certified by peer review) is the author/funder, who has granted bioRxiv a license to display the preprint in perpetuity. It is made available under aCC-BY 4.0 International license.

460 × 0.5 × 1 mm).

461

462 ***Image preprocessing***

463 Functional images were preprocessed using SPM12 (Wellcome Center for Human Neuroimaging,
464 London, UK, http://www.fil.ion.ucl.ac.uk/spm12/). For each participant, the first 4 volumes of each
465 functional run were discarded for signal equilibrium. The remaining images were corrected for slice
466 timing and head motion and then spatially normalized to Montreal Neurological Institute (MNI)
467 space via unified segmentation (resampling into 2 × 2 × 2 mm voxel size). All participants had head
468 motion less than 1.97 mm/1.95°, except for one hearing participant showing excessive head motion
469 in 2 runs (> 2 mm/2°); we thus analyzed the remaining 8 runs of fMRI data for this participant. We
470 also estimated each participant's framewise displacement (FD) from translations and rotations
471 (Power et al., 2012); the two deaf groups exhibited comparable FD during scanning (Native: 0.12 ±
472 0.04; Delayed: 0.11 ± 0.04; Welch's $t_{29.08}$ = 0.77, p = .45). Spatial smoothing was applied with a
473 Gaussian kernel of 6 mm full width at half maximum (FWHM) for univariate analysis and 2 mm
474 FWHM for representational similarity analysis (RSA).

475

476 ***ROI definition***

477 A GLM was built to localize semantic abstractness in the brain, i.e., brain regions showing stronger
478 activation to abstract/nonobject words than to concrete/object words, in hearing participants. For
479 spatially smoothed functional images, the GLM included 3 regressors (i.e., abstract/nonobject
480 words, concrete/object words, and catch trials) for each run, each convolved with the canonical
481 hemodynamic response function (HRF). The GLM also included six head motion parameters and a
482 global mean predictor of each run. The high-pass filter was set at 128 s. The contrast (i.e., abstract >
483 concrete) was computed for each participant.

bioRxiv preprint doi: https://doi.org/10.1101/2022.11.06.515336; this version posted November 7, 2022. The copyright holder for this preprint (which was not certified by peer review) is the author/funder, who has granted bioRxiv a license to display the preprint in perpetuity. It is made available under aCC-BY 4.0 International license.

The brain regions of semantic abstractness were considered as candidates supporting knowledge derived from language. These regions were functionally localized in hearing participants. The beta-weight images of abstract > concrete in hearing participants were submitted to one-sample *t*-tests. A conventional cluster-extent-based inference threshold (voxel-level $p < .001$, cluster-level FWE-corrected $p < .05$) was adopted and we stated explicitly when other thresholds were applied. At the conventional threshold, six clusters were found (Figure 1c and Figure 1-figure supplement 2). As the largest cluster extended from the left dATL to the left IFG, we separated the dATL (808 voxels) and IFG (411 voxels) into two ROIs based on the automated anatomical labeling (AAL) atlas (Tzourio-Mazoyer et al., 2002). To have the cluster sizes comparable across ROIs, we increased voxel-level threshold to $p < .0001$ and obtained a smaller dATL cluster (488 voxels), based on which the ROI-level results were reported; the results were largely similar across different sizes of the dATL ROI.

Representational similarity analysis in two deaf groups

GLM: The preprocessed functional images were analyzed using a GLM to create a *t*-statistic image for each word (Kriegeskorte et al., 2008a). For each participant, a GLM was built with the concatenated time series across all the scanning runs, including 90 regressors corresponding to each word and one regressor for catch trials, convolved with a canonical HRF. Additionally, 6 head motion parameters and a global mean predictor were included for each run. A high-pass filter cutoff was set as 128 s. The resulting *t*-maps for each word versus baseline were used to create neural RDMs.

ROI-level RSA: For each ROI in each participant, we extracted the activity patterns to each word

bioRxiv preprint doi: https://doi.org/10.1101/2022.11.06.515336; this version posted November 7, 2022. The copyright holder for this preprint (which was not certified by peer review) is the author/funder, who has granted bioRxiv a license to display the preprint in perpetuity. It is made available under aCC-BY 4.0 International license.

from its whole-brain t-statistic images and calculated a neural 90 × 90 RDM based on the Pearson distance between activation patterns for each pair of words. Semantic information encoded in this ROI was quantified by computing Spearman's rank correlation between the neural RDM and the 10-category benchmark semantic RDM. Partial correlations were used to control for two stimulus low-level property RDMs: (1) The low-level visual RDM was computed by Pearson's correlation distance between the binary silhouette images of each word pair. (2) The word phonological RDM: Despite that our task did not require explicit phonological retrieval, there might be automatic phonological activation. We thus constructed the phonological RDM by calculating one minus the proportion of shared sub-syllabic units (onsets or rhyme) between each word pair. The resulting correlation coefficients between neural and semantic RDMs were Fisher-*z*-transformed and compared with zero using one-sample t-tests (one-tailed) to test whether the ROI significantly encoded the semantic structure. Group differences in semantic encoding were assessed using two-tailed Welch's t-tests for each ROI.

Whole-brain searchlight RSA: To explore the potential differences between native and delayed signers in the neural semantic representations beyond the semantic ROIs identified above, we carried out whole-brain searchlight RSA. For each voxel in the AAL mask, we extracted the multivoxel activity patterns of 90 words within a sphere (radius = 8 mm) centered at that voxel. A neural 90 × 90 RDM was computed based on Pearson distance and was correlated with the semantic benchmark RDM while controlling for the two low-level RDMs of visual and phonological similarity of word stimuli, which produced a correlation coefficient for this voxel. By moving the searchlight center through the AAL mask, we obtained a correlation map for each participant. This map was Fisher-*z*-transformed and then spatially smoothed using a 6-mm FWHM Gaussian kernel. The correlation maps of native and delayed groups were compared using a two-sample *t*-test.

bioRxiv preprint doi: https://doi.org/10.1101/2022.11.06.515336; this version posted November 7, 2022. The copyright holder for this preprint (which was not certified by peer review) is the author/funder, who has granted bioRxiv a license to display the preprint in perpetuity. It is made available under aCC-BY 4.0 International license.

Univariate semantic abstractness analysis in two deaf groups

GLM: The neural semantic abstractness effects were computed using the same GLMs in the "ROI definition" section. For each deaf participant, we computed the following three contrasts for ROI and whole-brain group comparisons using all the runs: abstract > concrete, abstract words > baseline, concrete words > baseline.

ROI analysis: For each ROI, we extracted the averaged beta values of abstract words > baseline and concrete words > baseline, from each deaf participant, and compared between two word types using one-tailed paired *t*-tests to test for the semantic abstractness effects in each deaf group. Two-way ANOVA was then adopted to examine group effects, with word type (concrete/object, abstract/nonobject) as a within-subject factor and group (native, delayed) as a between-subject factor.

fROI analysis: We also carried out individualized functional Region-of-Interest (fROI) analyses (Cohen et al., 2019; Murty et al., 2020), which examined semantic selectivity in individually defined functional voxels, with the fROI localization and selectivity calculation using independent datasets. Specifically, we estimated each deaf participant's whole-brain beta and *t* maps for the contrast between abstract/nonobject and concrete/object words in odd and even runs. The semantic ROIs defined above in hearing participants were taken as anatomical constraints. In each hearing-group-ROI, for each deaf participant, we localized his/her top 50 selective voxels (i.e., voxels with highest *t* values to the contrast) in the odd runs, extracted the mean beta values of these voxels to abstract and concrete words, respectively, in the even runs. This procedure was repeated with fROI defined in the even runs and beta values calculated in the odd runs. The beta values were

bioRxiv preprint doi: https://doi.org/10.1101/2022.11.06.515336; this version posted November 7, 2022. The copyright holder for this preprint (which was not certified by peer review) is the author/funder, who has granted bioRxiv a license to display the preprint in perpetuity. It is made available under aCC-BY 4.0 International license.

556 averaged across two iterations for each ROI in each participant and compared between two deaf
557 groups using the abovementioned statistical analyses. We also repeated the fROI analyses at the
558 fROI size of 100 voxels and obtained very similar results.
559
560 *Whole-brain group comparison*: The whole-brain semantic abstractness effects were examined in
561 each deaf group, by one-sample *t*-tests on the whole-brain beta-weight images of abstract >
562 concrete in each group. For the interaction between group (native, delayed) and word-type
563 (abstract, concrete), the abstract > concrete beta-weight maps of two deaf groups were submitted
564 to a two-sample *t*-test.
565
566 ***Brain visualization***
567 The brain results were projected onto the MNI brain surface for visualization using BrainNet Viewer
568 (version 1.7; https://www.nitrc.org/projects/bnv/; (Xia et al., 2013)) with the default "interpolated"
569 mapping algorithm, unless stated explicitly otherwise. Regional labels were derived based on the
570 AAL template in xjview (by Xu Cui, http://www. alivelearn.net/xjview/).
571
572 **Data availability**
573 Source data files have been provided for Table 1 and all the figures. Additional behavioral and
574 neural data have been made available on OSF at the link https://osf.io/wz6q9/.
575

bioRxiv preprint doi: https://doi.org/10.1101/2022.11.06.515336; this version posted November 7, 2022. The copyright holder for this preprint (which was not certified by peer review) is the author/funder, who has granted bioRxiv a license to display the preprint in perpetuity. It is made available under aCC-BY 4.0 International license.

Acknowledgments: We thank Dr. Xi Yu for helpful discussions on earlier drafts of the manuscript. We thank Ms. Yun Hao, Anran Deng, and Wei Liang for their assistance in data collection. This work was supported by the National Science and Technology Innovation 2030 Major Program (2021ZD0204104), the National Natural Science Foundation of China (31925020 and 82021004 to Y.B, 31700943 and 32171052 to X.W.), and Changjiang Scholar Professorship Award (T2016031 to Y.B.). The funders had no role in study design, data collection and analysis, decision to publish, or preparation of the manuscript.

Competing interests: Yanchao Bi is a Reviewing editor of *eLife.* Other authors declare that no competing interests exist.

Supplementary files:

- Supplementary file 1. Behavioral performances of two deaf groups in two reaction-time tasks.
- Supplementary file 2. Whole-brain RSA results of pixelwise similarity of visual words in two deaf groups.

bioRxiv preprint doi: https://doi.org/10.1101/2022.11.06.515336; this version posted November 7, 2022. The copyright holder for this preprint (which was not certified by peer review) is the author/funder, who has granted bioRxiv a license to display the preprint in perpetuity. It is made available under aCC-BY 4.0 International license.

References

Adler NE, Epel ES, Castellazzo G, Ickovics JR. 2000. Relationship of subjective and objective social status with psychological and physical health in healthy white women. *Heal Psychol* **19**:586–592.

Barsalou LW. 2016. On Staying Grounded and Avoiding Quixotic Dead Ends. *Psychon Bull Rev* **23**:1122–1142. doi:10.3758/s13423-016-1028-3

Baus C, Gutiérrez-Sigut E, Quer J, Carreiras M. 2008. Lexical access in Catalan Signed Language (LSC) production. *Cognition* **108**:856–865. doi:10.1016/j.cognition.2008.05.012

Bi Y. 2021. Dual coding of knowledge in the human brain. *Trends Cogn Sci* **25**:883–895. doi:10.1016/j.tics.2021.07.006

Binder JR. 2016. In defense of abstract conceptual representations. *Psychon Bull Rev* **23**:1096–1108. doi:10.3758/s13423-015-0909-1

Binder JR, Conant LL, Humphries CJ, Fernandino L, Simons SB, Aguilar M, Desai RH. 2016. Toward a brain-based componential semantic representation. *Cogn Neuropsychol* **33**:130–174. doi:10.1080/02643294.2016.1147426

Binder JR, Desai RH. 2011. The neurobiology of semantic memory. *Trends Cogn Sci* **15**:527–536. doi:10.1016/j.tics.2011.10.001

Binder JR, Desai RH, Graves WW, Conant LL. 2009. Where is the semantic system? A critical review and meta-analysis of 120 functional neuroimaging studies. *Cereb Cortex* **19**:2767–2796. doi:10.1093/cercor/bhp055

Bogliotti C, Aksen H, Isel F. 2020. Language experience in LSF development: Behavioral evidence from a sentence repetition task. *PLoS One* **15**:1–26. doi:10.1371/journal.pone.0236729

Bottini R, Ferraro S, Nigri A, Cuccarini V, Bruzzone MG, Collignon O. 2020. Brain regions involved in conceptual retrieval in sighted and blind people. *J Cogn Neurosci* **32**:1009–1025. doi:10.1162/jocn_a_01538

Bucur M, Papagno C. 2021. An ALE meta-analytical review of the neural correlates of abstract and concrete words. *Sci Rep* **11**:1–24. doi:10.1038/s41598-021-94506-9

Caselli NK, Emmorey K, Cohen-Goldberg AM. 2021. The signed mental lexicon: Effects of phonological neighborhood density, iconicity, and childhood language experience. *J Mem Lang* **121**:104282. doi:10.1016/j.jml.2021.104282

Cheng Q, Mayberry RI. 2021. When event knowledge overrides word order in sentence comprehension: Learning a first language after childhood. *Dev Sci* **24**:e13073. doi:10.1111/desc.13073

Cheng Q, Roth A, Halgren E, Mayberry RI. 2019. Effects of Early Language Deprivation on Brain Connectivity: Language Pathways in Deaf Native and Late First-Language Learners of American Sign Language. *Front Hum Neurosci* **13**:1–12. doi:10.3389/fnhum.2019.00320

Cohen MA, Dilks DD, Koldewyn K, Weigelt S, Feather J, Kell AJ, Keil B, Fischl B, Zöllei L, Wald L, Saxe R, Kanwisher N. 2019. Representational similarity precedes category selectivity in the developing ventral visual pathway. *Neuroimage* **197**:565–574. doi:10.1016/j.neuroimage.2019.05.010

Conca F, Borsa VM, Cappa SF. 2021. The multidimensionality of abstract concepts: A systematic review. *Neurosci Biobehav Rev* **127**:474–491. doi:10.1016/j.neubiorev.2021.05.004

Davidson K, Mayberry RI. 2015. Do Adults Show an Effect of Delayed First Language Acquisition When Calculating Scalar Implicatures? *Lang Acquis* **22**:329–354. doi:10.1080/10489223.2014.962140

Fan L, Wang J, Zhang Y, Han W, Yu C, Jiang T. 2014. Connectivity-based parcellation of the human temporal pole using diffusion tensor imaging. *Cereb Cortex* **24**:3365–3378. doi:10.1093/cercor/bht196

Farahibozorg S-R, Henson RN, Woollams AM, Hauk O. 2022. Distinct Roles for the Anterior Temporal Lobe

bioRxiv preprint doi: https://doi.org/10.1101/2022.11.06.515336; this version posted November 7, 2022. The copyright holder for this preprint (which was not certified by peer review) is the author/funder, who has granted bioRxiv a license to display the preprint in perpetuity. It is made available under aCC-BY 4.0 International license.

636 and Angular Gyrus in the Spatiotemporal Cortical Semantic Network. *Cereb Cortex* 1–16.
637 doi:10.1093/cercor/bhab501
638 Fernandino L, Tong JQ, Conant LL, Humphries CJ, Binder JR. 2022. Decoding the information structure
639 underlying the neural representation of concepts. *Proc Natl Acad Sci U S A* **119**:1–11.
640 doi:10.1073/pnas.2108091119
641 Friederici AD, Chomsky N, Berwick RC, Moro A, Bolhuis JJ. 2017. Language, mind and brain. *Nat Hum Behav*
642 **1**:713–722. doi:10.1038/s41562-017-0184-4
643 Fu Z, Wang Xiaosha, Wang Xiaoying, Yang H, Wang J, Wei T, Liao X, Liu Z, Chen H, Bi Y. 2022. Different
644 computational relations in language are captured by distinct brain systems. *Cereb Cortex* 1–17.
645 doi:10.1093/cercor/bhac117
646 Gelman SA, Roberts SO. 2017. How language shapes the cultural inheritance of categories. *Proc Natl Acad Sci*
647 *U S A* **114**:7900–7907. doi:10.1073/pnas.1621073114
648 Goldin-Meadow S. 2003. The Resilience of Language: What gesture creation in deaf children can tell us
649 about how all children learn language. New York: Psychology Press.
650 Goldin-Meadow S, Feldman H. 1977. The development of language-like communication without a language
651 model. *Science (80-)* **197**:401–403. doi:10.1126/science.877567
652 Goldin-Meadow S, Gelman SA, Mylander C. 2005. Expressing generic concepts with and without a language
653 model. *Cognition* **96**:109–126. doi:10.1016/j.cognition.2004.07.003
654 Kriegeskorte N, Goebel R, Bandettini P. 2006. Information-based functional brain mapping. *Proc Natl Acad*
655 *Sci U S A* **103**:3863–3868. doi:10.1073/pnas.0600244103
656 Kriegeskorte N, Mur M. 2012. Inverse MDS: Inferring dissimilarity structure from multiple item arrangements.
657 *Front Psychol* **3**:1–13. doi:10.3389/fpsyg.2012.00245
658 Kriegeskorte N, Mur M, Bandettini P. 2008a. Representational similarity analysis - connecting the branches
659 of systems neuroscience. *Front Syst Neurosci* **2**:1–28. doi:10.3389/neuro.06.004.2008
660 Kriegeskorte N, Mur M, Ruff DA, Kiani R, Bodurka J, Esteky H, Tanaka K, Bandettini PA. 2008b. Matching
661 Categorical Object Representations in Inferior Temporal Cortex of Man and Monkey. *Neuron* **60**:1126–
662 1141. doi:10.1016/j.neuron.2008.10.043
663 Lambon Ralph MA, Jefferies E, Patterson K, Rogers TT. 2017. The neural and computational bases of
664 semantic cognition. *Nat Rev Neurosci* **18**:42–55. doi:10.1038/nrn.2016.150
665 Lefly DL, Pennington BF. 2000. Reliability and validity of the adult reading history questionnaire. *J Learn*
666 *Disabil* **33**:286–296. doi:10.1177/002221940003300306
667 Lieberman AM, Borovsky A, Hatrak M, Mayberry RI. 2015. Real-time processing of ASL signs: Delayed first
668 language acquisition affects organization of the mental lexicon. *J Exp Psychol Learn Mem Cogn*
669 **41**:1130–1139. doi:10.1037/xlm0000088
670 Lupyan G, Abdel Rahman R, Boroditsky L, Clark A. 2020. Effects of Language on Visual Perception. *Trends*
671 *Cogn Sci* **24**:930–944. doi:10.1016/j.tics.2020.08.005
672 MacSweeney M, Waters D, Brammer MJ, Woll B, Goswami U. 2008. Phonological processing in deaf signers
673 and the impact of age of first language acquisition. *Neuroimage* **40**:1369–1379.
674 doi:10.1016/j.neuroimage.2007.12.047
675 Mahon BZ, Caramazza A. 2008. A critical look at the embodied cognition hypothesis and a new proposal for
676 grounding conceptual content. *J Physiol Paris* **102**:59–70. doi:10.1016/j.jphysparis.2008.03.004
677 Marshall C, Jones A, Denmark T, Mason K, Atkinson J, Botting N, Morgan G. 2015. Deaf children's non-verbal
678 working memory is impacted by their language experience. *Front Psychol* **6**:1–12.
679 doi:10.3389/fpsyg.2015.00527

bioRxiv preprint doi: https://doi.org/10.1101/2022.11.06.515336; this version posted November 7, 2022. The copyright holder for this preprint (which was not certified by peer review) is the author/funder, who has granted bioRxiv a license to display the preprint in perpetuity. It is made available under aCC-BY 4.0 International license.

680 Martin A. 2016. GRAPES—Grounding representations in action, perception, and emotion systems: How
681 object properties and categories are represented in the human brain. *Psychon Bull Rev* **23**:979–990.
682 doi:10.3758/s13423-015-0842-3
683 Mayberry RI, Chen JK, Witcher P, Klein D. 2011. Age of acquisition effects on the functional organization of
684 language in the adult brain. *Brain Lang* **119**:16–29. doi:10.1016/j.bandl.2011.05.007
685 Mayberry RI, Davenport T, Roth A, Halgren E. 2018. Neurolinguistic processing when the brain matures
686 without language. *Cortex* **99**:390–403. doi:10.1016/j.cortex.2017.12.011
687 Mayberry RI, Fischer SD. 1989. Looking through phonological shape to lexical meaning: The bottleneck of
688 non-native sign language processing. *Mem Cognit* **17**:740–754. doi:10.3758/BF03202635
689 Mayberry RI, Lock E, Kazmi H. 2002. Linguistic ability and early language exposure. *Nature* **417**:38.
690 doi:10.1038/417038a
691 Murty NAR, Teng S, Beeler D, Mynick A, Oliva A, Kanwisher N. 2020. Visual experience is not necessary for
692 the development of face-selectivity in the lateral fusiform gyrus. *Proc Natl Acad Sci U S A* **117**:23011–
693 23020. doi:10.1073/pnas.2004607117
694 Newport EL. 1990. Maturational constraints on language development. *Cogn Sci* **14**:11–28.
695 Oldfield R. 1971. The assessment and analysis of handedness: the Edinburgh inventory. *Neuropsychologia*
696 **9**:97–113.
697 Pallier C, Devauchelle AD, Dehaene S. 2011. Cortical representation of the constituent structure of sentences.
698 *Proc Natl Acad Sci U S A* **108**:2522–2527. doi:10.1073/pnas.1018711108
699 Pascual B, Masdeu JC, Hollenbeck M, Makris N, Insausti R, Ding SL, Dickerson BC. 2015. Large-scale brain
700 networks of the human left temporal pole: A functional connectivity MRI study. *Cereb Cortex* **25**:680–
701 702. doi:10.1093/cercor/bht260
702 Patterson K, Nestor PJ, Rogers TT. 2007. Where do you know what you know? The representation of
703 semantic knowledge in the human brain. *Nat Rev Neurosci* **8**:976–987. doi:10.1038/nrn2277
704 Perszyk DR, Waxman SR. 2018. Linking Language and Cognition in Infancy. *Annu Rev Psychol* **69**:10.1-10.20.
705 doi:10.1093/cercor/bhv082
706 Power JD, Barnes KA, Snyder AZ, Schlaggar BL, Petersen SE. 2012. Spurious but systematic correlations in
707 functional connectivity MRI networks arise from subject motion. *Neuroimage* **59**:2142–2154.
708 doi:10.1016/j.neuroimage.2011.10.018
709 Pylkkänen L. 2019. The neural basis of combinatory syntax and semantics. *Science (80-)*.
710 doi:10.1126/science.aax0050
711 Richardson H, Koster-Hale J, Caselli N, Magid R, Benedict R, Olson H, Pyers J, Saxe R. 2020. Reduced neural
712 selectivity for mental states in deaf children with delayed exposure to sign language. *Nat Commun*
713 **11**:1–13. doi:10.1038/s41467-020-17004-y
714 Skotara N, Salden U, Kügow M, Hänel-Faulhaber B, Röder B. 2012. The influence of language deprivation in
715 early childhood on L2 processing: An ERP comparison of deaf native signers and deaf signers with a
716 delayed language acquisition. *BMC Neurosci* **13**. doi:10.1186/1471-2202-13-44
717 Spelke ES. 2017. Core Knowledge, Language, and Number. *Lang Learn Dev* **13**:147–170.
718 doi:10.1080/15475441.2016.1263572
719 Striem-Amit E, Wang X, Bi Y, Caramazza A. 2018. Neural representation of visual concepts in people born
720 blind. *Nat Commun* **9**:5250. doi:10.1038/s41467-018-07574-3
721 Sun H, Huang J, Sun D, Li D, Xing H. 1997. Introduction to language corpus system of modern Chinese study
722 In: Hu MY, editor. Paper Collection for the Fifth World Chinese Teaching Symposium. Beijing: Peking
723 University Publishers. pp. 459–66.

bioRxiv preprint doi: https://doi.org/10.1101/2022.11.06.515336; this version posted November 7, 2022. The copyright holder for this preprint (which was not certified by peer review) is the author/funder, who has granted bioRxiv a license to display the preprint in perpetuity. It is made available under aCC-BY 4.0 International license.

Tibshirani R, Walther G, Hastie T. 2001. Estimating the number of clusters in a data set via the gap statistic. *J R Stat Soc B* **63**:411–423.

Tomaszewski P, Krzysztofiak P, Morford JP, Eźlakowski W. 2022. Effects of Age-of-Acquisition on Proficiency in Polish Sign Language: Insights to the Critical Period Hypothesis. *Front Psychol* **13**:1–16. doi:10.3389/fpsyg.2022.896339

Twomey T, Price CJ, Waters D, MacSweeney M. 2020. The impact of early language exposure on the neural system supporting language in deaf and hearing adults. *Neuroimage* **209**:116411. doi:10.1016/j.neuroimage.2019.116411

Tzourio-Mazoyer N, Landeau B, Papathanassiou D, Crivello F, Etard O, Delcroix N, Mazoyer B, Joliot M. 2002. Automated anatomical labeling of activations in SPM using a macroscopic anatomical parcellation of the MNI MRI single-subject brain. *Neuroimage* **15**:273–289. doi:10.1006/nimg.2001.0978

Unger L, Fisher A V. 2021. The emergence of richly organized semantic knowledge from simple statistics: A synthetic review. *Dev Rev* **60**:100949. doi:10.1016/j.dr.2021.100949

Wang J, Conder JA, Blitzer DN, Shinkareva S V. 2010. Neural representation of abstract and concrete concepts: A meta-analysis of neuroimaging studies. *Hum Brain Mapp* **31**:1459–1468. doi:10.1002/hbm.20950

Wang X, Bi Y. 2021. Idiosyncratic tower of babel: Individual differences in word meaning representation increase along abstractness. *Psychol Sci* **32**:1617–1635.

Wang X, Men W, Gao J, Caramazza A, Bi Y. 2020. Two Forms of Knowledge Representations in the Human Brain. *Neuron* **107**:383-393.e5. doi:10.1016/j.neuron.2020.04.010

Wang X, Wang B, Bi Y. 2019. Close yet independent: Dissociation of social from valence and abstract semantic dimensions in the left anterior temporal lobe. *Hum Brain Mapp* **40**:4759–4776. doi:10.1002/hbm.24735

Wei T, Liang X, He Y, Zang Y, Han Z, Caramazza A, Bi Y. 2012. Predicting conceptual processing capacity from spontaneous neuronal activity of the left middle temporal gyrus. *J Neurosci* **32**:481–489. doi:10.1523/JNEUROSCI.1953-11.2012

Xia M, Wang J, He Y. 2013. BrainNet Viewer: A Network Visualization Tool for Human Brain Connectomics. *PLoS One* **8**:e68910. doi:10.1371/journal.pone.0068910

Xu Y, He Y, Bi Y. 2017. A tri-network model of human semantic processing. *Front Psychol* **8**:1538. doi:10.3389/fpsyg.2017.01538

bioRxiv preprint doi: https://doi.org/10.1101/2022.11.06.515336; this version posted November 7, 2022. The copyright holder for this preprint (which was not certified by peer review) is the author/funder, who has granted bioRxiv a license to display the preprint in perpetuity. It is made available under aCC-BY 4.0 International license.

Figure legends

Figure 1. The word stimuli, task fMRI procedure, and ROIs in this study. **a.** Word stimuli in the task fMRI. Ninety words were used, including 40 concrete/object words and 50 abstract/nonobject words, which were grouped into fine-grained categories based on k-means clustering of the group-averaged semantic space of 32 hearing participants. The left panel shows the group-averaged semantic representational matrices (RDM) in hearing participants, native signers, and delayed signers. The right panel shows the Spearman's rho between each deaf participant's semantic RDM and the group-averaged semantic RDM in hearing participants. **b.** Task fMRI procedure. During scanning, participants were asked to think about each of 90 target word meanings (displayed in black, e.g., "panda", "reason") and to determine whether occasional words displayed in red (catch trials, e.g., "justification") were semantically related to the previous word. There were 90 target word trials (each word appeared once) and 14 catch trials in each run. **c.** Semantic ROIs were functionally identified by contrasting abstract/nonobject words with concrete/object words in 33 hearing participants at the threshold of voxel-level $p < .001$, cluster-level FWE-corrected $p < .05$. dATL, dorsal anterior temporal lobe; IFG, inferior frontal gyrus; pMTG, posterior middle temporal gyrus. L, left hemisphere; R, right hemisphere.

The following source data and figure supplement are available for figure 1:

Source data 1: Spearman's rho between each deaf participant's semantic RDM and the group-averaged semantic RDM in hearing participants.

Figure supplement 1. Ninety words in the fMRI task, grouped into ten semantic categories.

Figure supplement 2. Details of semantic ROIs, including cluster location, extent, peak t values, and MNI coordinates.

Figure supplement 3. RSA and univariate results in other ROIs (except for the left dATL, IFG, and pMTG) in two deaf groups.

Figure 2. Effects of early language deprivation on neural representations of semantic knowledge. **a.** RSA procedure. For each participant, a neural RDM was computed as the correlation distance of multivoxel activity patterns (in a given ROI) for each pair of words and then correlated with the hearing-group-level semantic category RDM to quantify semantic information encoded in the neural RDM. **b.** ROI-level RSA results. Error bars indicate 1 s.e.m. n.s., not significant, $p > .05$; *, $p < .05$; **, $p < .01$; ***, $p < .001$; **c.** Whole-brain searchlight RSA results. The statistical maps were thresholded at voxel-level $p < .001$, cluster FWE-corrected $p < .05$, for native signers and at voxel-level $p < .001$, cluster size > 10 voxels, for delayed signers and group comparisons. Brain results of group comparisons and delayed signers were visualized using the "Maximum Voxel" mapping algorithm in BrainNet Viewer to illustrate small clusters. Clusters in the left hemisphere are shown here. n = 16 in the native group; n = 23 in the delayed group.

The following source data and figure supplement are available for figure 2:

Source data 1: ROI-level RSA results in two deaf groups.

Figure supplement 1. Cluster details of whole-brain searchlight RSA results.

Figure 3. Effects of early language deprivation on the univariate semantic abstractness effects in group-level-defined semantic ROIs (**a**) and individual fROIs (**b**). Boxplots show beta values to abstract/nonobject words and concrete/object words in the three ROIs (the left dATL, pMTG, and

bioRxiv preprint doi: https://doi.org/10.1101/2022.11.06.515336; this version posted November 7, 2022. The copyright holder for this preprint (which was not certified by peer review) is the author/funder, who has granted bioRxiv a license to display the preprint in perpetuity. It is made available under aCC-BY 4.0 International license.

IFG). n.s., not significant, $p > .05$; *, $p < .05$; **, $p < .01$; ***, $p < .001$. n = 16 in the native group; n = 23 in the delayed group.

The following source data and figure supplement are available for figure 3:

Source data 1: Raw beta values to abstract/nonobject words and concrete/object words in group-level-defined semantic ROIs and individual fROIs in two deaf groups.

Figure supplement 1. Whole-brain univariate results of semantic abstractness in native and delayed signers.

bioRxiv preprint doi: https://doi.org/10.1101/2022.11.06.515336; this version posted November 7, 2022. The copyright holder for this preprint (which was not certified by peer review) is the author/funder, who has granted bioRxiv a license to display the preprint in perpetuity. It is made available under aCC-BY 4.0 International license.

Table 1. Background demographic and language information of native and delayed signers.

	native (n = 16)	delayed (n = 23)	Welch's t	*p*-value	Hedges' g
AoA of CSL (years old)	0 ± 0	6.91 ± 1.62			
Parental CSL proficiency (1-7 scale) [a] **	6.81 ± 0.54	2.74 ± 1.29	13.54	<.001	4.04
Gender	11M, 5F	12M, 11F			
Age (years)	28.50 ± 7.13	27.09 ± 5.87	0.65	.52	0.21
Education (years)	14.13 ± 2.31	15.09 ± 1.41	-1.49	.15	-0.49
CSL comprehension (1-7 scale) [a]	6.06 ± 0.93	6.17 ± 0.89	-0.38	.71	-0.12
CSL production (1-7 scale) [a]	5.75 ± 1.00	5.87 ± 1.10	-0.35	.73	-0.11
Lipreading of acquaintances (1-7 scale) [a]	2.81 ± 1.11	3.17 ± 1.19	-0.97	.34	-0.31
Lipreading of strangers (1-7 scale) [a]	1.88 ± 0.81	1.87 ± 0.97	0.02	.99	0.01
Adult Reading History Questionnaire (0-4 scale) [b]	2.59 ± 0.68	2.84 ± 0.52	-1.25	.22	-0.41
McArthur Scale of Subjective Social Status, childhood (1-10 scale) [c]	3.88 ± 2.58	4.35 ± 1.97	-0.62	.54	-0.20
Father's education (years)	7.19 ± 3.04	10.39 ± 2.84	-2.02	.053	-0.65
Mother's education (years)**	6.56 ± 3.14	8.52 ± 2.73	-3.33	.002	-1.07

Notes:

a: higher scores indicate higher proficiency.

b: higher scores indicate higher risk of reading disability; from (Lefly and Pennington, 2000).

c: higher scores indicate higher social status; from (Adler et al., 2000).

**: $p < .01$, significant differences between 2 deaf groups.

The following source data is available for Table 1:

Source data 1: Background demographic and language information of native and delayed signers.

Figure 1

a Word stimuli in the task fMRI

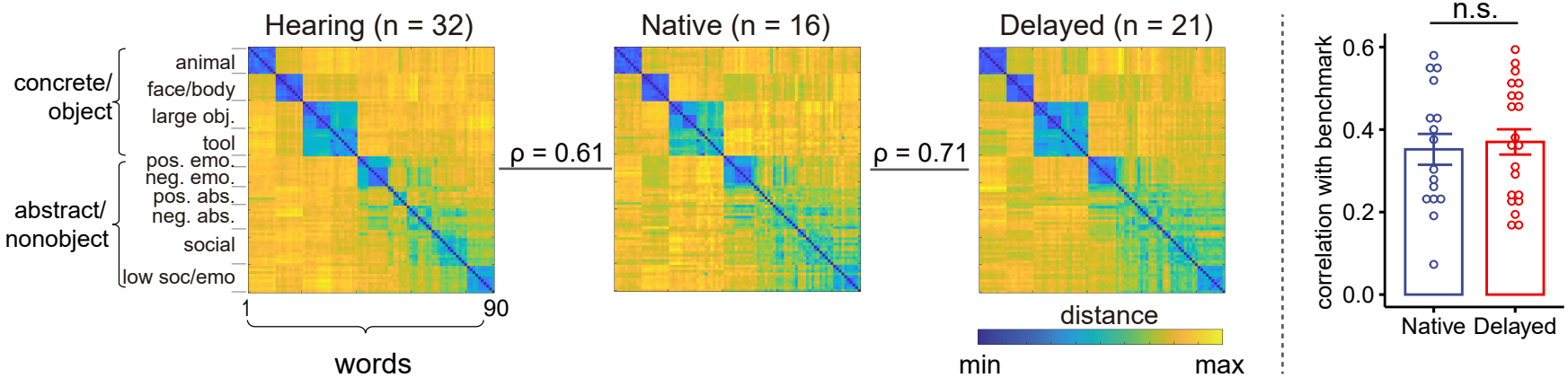

b Task fMRI procedure

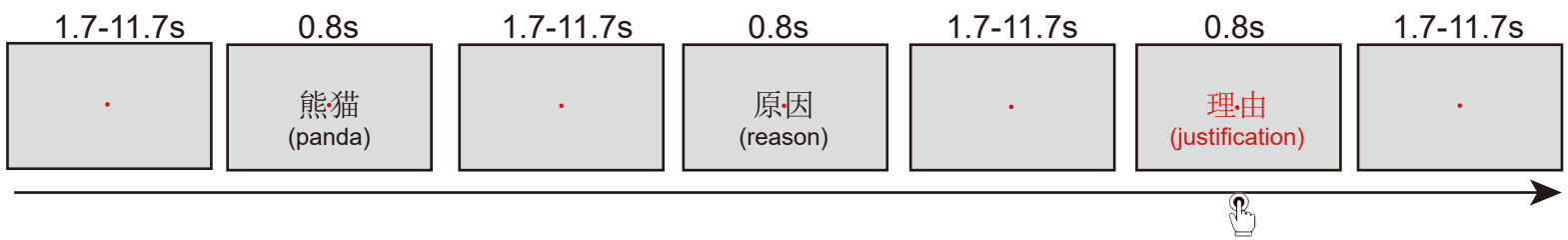

c ROIs with abstractness effects in hearing

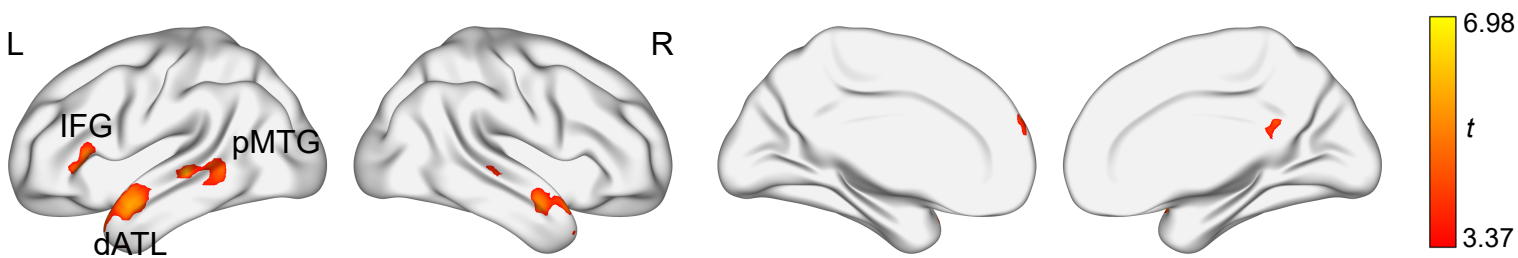

Figure 2

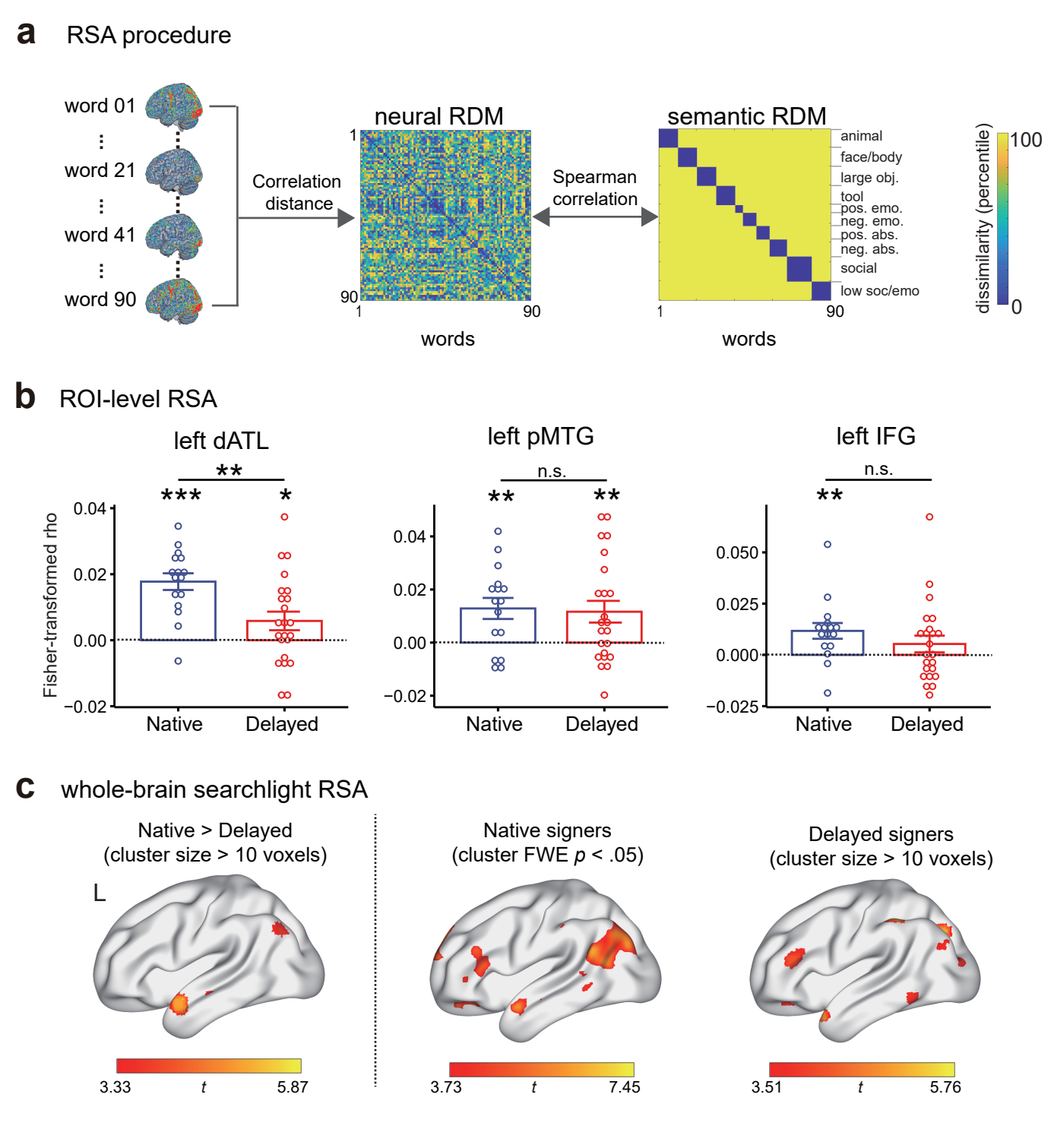
a
RSA procedure
word 01
word 21
word 41
word 90
Correlation distance
neural RDM
1
90
1
90
words
Spearman correlation
semantic RDM
animal
face/body
large obj.
tool
pos. emo.
neg. emo.
pos. abs.
neg. abs.
social
low soc/emo
1
90
words
dissimilarity (percentile)
100
0
b
ROI-level RSA
left dATL
left pMTG
left lFG
Fisher-transformed rho
0.04
0.02
0.00
−0.02
**
***
*
n.s.
**
**
n.s.
**
0.050
0.025
0.000
−0.025
Native
Delayed
c
whole-brain searchlight RSA
Native > Delayed
(cluster size > 10 voxels)
L
3.33
t
5.87
Native signers
(cluster FWE p < .05)
3.73
t
7.45
Delayed signers
(cluster size > 10 voxels)
3.51
t
5.76

Figure 3

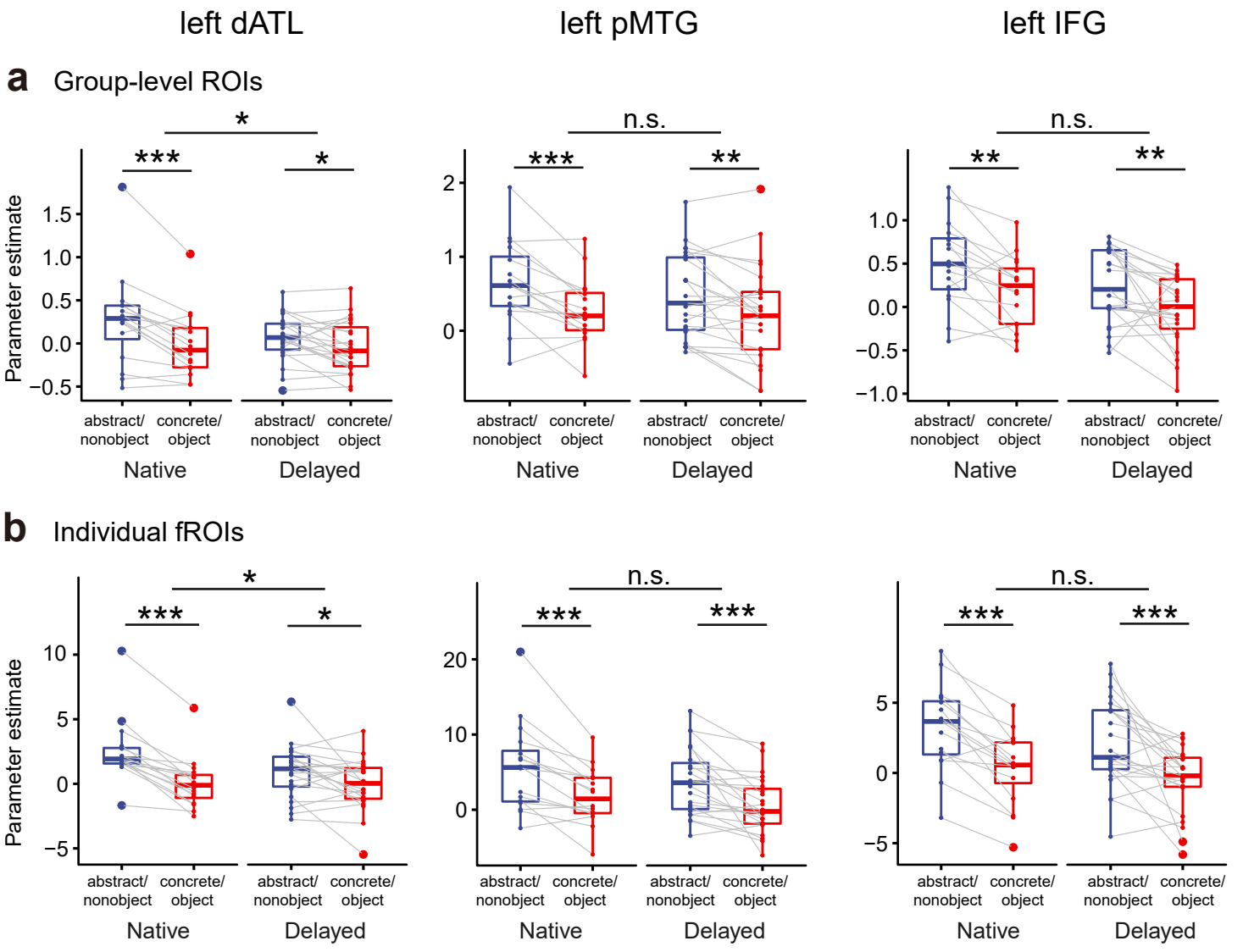
left dATL
left pMTG
left IFG
a Group-level ROIs
b Individual fROIs
Parameter estimate
*
***
*
n.s.
**
n.s.
**
abstract/ nonobject
concrete/ object
Native
Delayed

bioRxiv preprint doi: https://doi.org/10.1101/2022.11.06.515336; this version posted November 7, 2022. The copyright holder for this preprint (which was not certified by peer review) is the author/funder, who has granted bioRxiv a license to display the preprint in perpetuity. It is made available under aCC-BY 4.0 International license.

Figure 1-Figure supplement 1

Ninety words in the fMRI task, grouped into ten semantic clusters based on k-means clustering of the group-mean hearing semantic space.

No.	Cluster labels	Words
Cluster 1	Animals	熊猫 (panda), 老鼠 (rat), 老虎 (tiger), 大象 (elephant), 麻雀 (sparrow), 乌龟 (tortoise), 蚂蚁 (ant), 兔子 (rabbit), 猫 (cat), 长颈鹿 (giraffe)
Cluster 2	Face/Body parts	肩膀 (shoulder), 胳膊 (arm), 大腿 (thigh), 鼻子 (nose), 眼睛 (eye), 嘴唇 (lips), 耳朵 (ear), 膝盖 (knee), 手指 (finger), 脚踝 (ankle)
Cluster 3	Large objects	空调 (air conditioner), 冰箱 (refrigerator), 电视 (television), 微波炉 (microwave), 洗衣机 (washing machine), 柜子 (cabinet), 椅子 (chair), 沙发 (sofa), 桌子 (table), 床 (bed)
Cluster 4	Tools	勺子 (spoon), 剪刀 (scissors), 斧头 (axe), 鼠标 (computer mouse), 筷子 (chopsticks), 扫帚 (broom), 牙刷 (toothbrush), 钥匙 (key), 铅笔 (pencil), 锤子 (hammer)
Cluster 5	Positive emotions	兴奋 (excited), 舒心 (comfortable), 快乐 (happy), 骄傲 (proud)
Cluster 6	Negative emotions	敌意 (hostility), 愤怒 (anger), 恐惧 (fear), 冷漠 (apathy), 难过 (sad), 反感 (antipathy), 沮丧 (depressed)
Cluster 7	Positive abstract words	爱心 (loving/caring), 慈善 (charity), 魔力 (magic power), 奇迹 (miracle), 风景 (scenery), 天堂 (heaven), 光彩 (splendor)
Cluster 8	Negative abstract words	暴力 (violence), 骗局 (fraud), 纠纷 (dispute), 债务 (debt), 创伤 (trauma), 疾病 (disease), 死亡 (death), 过失 (fault), 错误 (error)
Cluster 9	Social words	缘分 (fate), 友情 (friendship), 婚姻 (marriage), 制度 (system), 社会 (society), 关系 (relationship), 地位 (status), 身份 (identity), 义务 (obligation), 买卖 (business), 协议 (agreement), 团队 (team), 纪律 (discipline)
Cluster 10	Low-emotional, low-social	概念 (concept), 内容 (content), 性质 (characteristic), 数据 (data), 作用 (effect), 结果 (result), 原因 (reason), 过程 (process), 方法 (method), 现象 (phenomenon)

bioRxiv preprint doi: https://doi.org/10.1101/2022.11.06.515336; this version posted November 7, 2022. The copyright holder for this preprint (which was not certified by peer review) is the author/funder, who has granted bioRxiv a license to display the preprint in perpetuity. It is made available under aCC-BY 4.0 International license.

Figure 1-Figure supplement 2

Whole-brain results of regions showing stronger activations to abstract/nonobject words than concrete/object words in 33 hearing participants.

Cluster name	Brodmann area	Cluster extent (voxels)	Peak *t* value	Maxima MNI coordinates		
				x	y	z
L TPOsup, IFGtriang, MTG, STG, ORBinf, TPOmid, ITG	38/21/47/45	1297	6.98	-48	16	-18
			5.88	-54	0	-16
			5.85	-52	24	6
R TPOsup, MTG, TPOmid, STG	38/21	746	6.30	58	10	-16
			5.83	56	0	-18
			5.64	42	10	-20
L MTG	21/22	516	6.09	-54	-28	0
			5.13	-52	-42	0
			4.95	-60	-46	0
L SFGmed	10/9	115	5.06	-6	60	28
			4.07	-8	60	20
B PCG, R PCUN	31/23	119	4.89	2	-46	24
			4.34	6	-42	16
R STG, MTG	22	109	4.68	50	-26	0
			4.15	58	-28	0
			3.83	44	-38	2

Notes: Clusters were reported at the threshold of voxel-level $p < .001$, cluster-level FWE-corrected $p < .05$. Two or three local maxima more than 8.0 mm apart were shown. L, left hemisphere; R, right hemisphere; B, bilateral. IFGtriang, inferior frontal gyrus, triangular part; ITG, inferior temporal gyrus; MTG, middle temporal gyrus; ORBinf, inferior frontal gyrus, orbital part; PCG, posterior cingulate gyrus; PCUN, precuneus; SFGmed, superior frontal gyrus, medial; STG, superior temporal gyrus; TPOmid, temporal pole: middle temporal gyrus; TPOsup, temporal pole: superior temporal gyrus.

bioRxiv preprint doi: https://doi.org/10.1101/2022.11.06.515336; this version posted November 7, 2022. The copyright holder for this preprint (which was not certified by peer review) is the author/funder, who has granted bioRxiv a license to display the preprint in perpetuity. It is made available under aCC-BY 4.0 International license.

Figure 1-Figure supplement 3

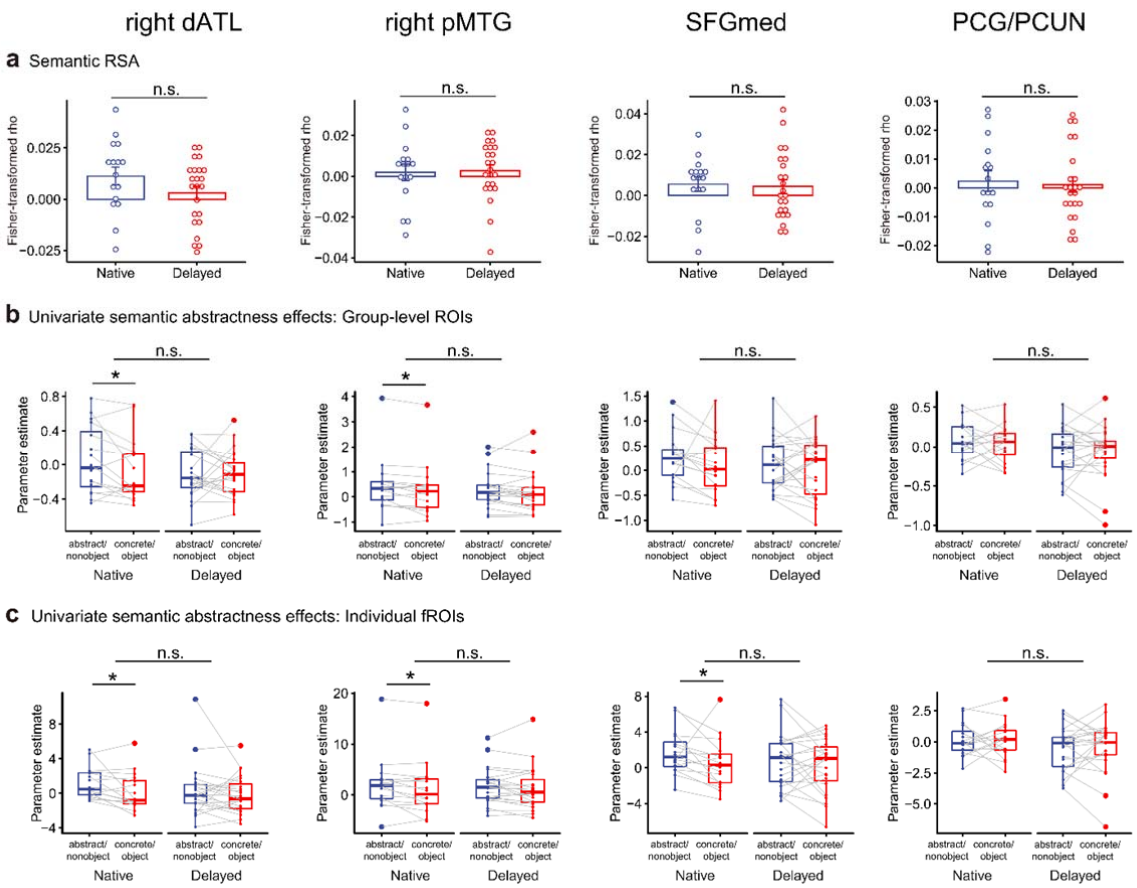

Additional ROI-level RSA (**a**) and univariate semantic abstractness results (**b** and **c**) in native and delayed signers. dATL, dorsal anterior temporal lobe; pMTG, posterior middle temporal gyrus; SFGmed, superior frontal gyrus, medial; PCG, posterior cingulate gyrus; PCUN, precuneus. n.s., not significant, $p > .05$; *, $p < .05$. n = 16 in the native group; n = 23 in the delayed group.

bioRxiv preprint doi: https://doi.org/10.1101/2022.11.06.515336; this version posted November 7, 2022. The copyright holder for this preprint (which was not certified by peer review) is the author/funder, who has granted bioRxiv a license to display the preprint in perpetuity. It is made available under aCC-BY 4.0 International license.

Figure 2-Figure supplement 1

Whole-brain searchlight RSA results of semantic encoding.

Cluster name	Cluster extent (voxels)	Cluster-level p (FWE corrected)	Peak *t* value	Maxima MNI coordinates		
				x	y	z
Native > delayed (df = 37)						
L MTG, TPOsup	162	0.22	5.87	-60	6	-20
L SFGmed, SFGdor	114	0.38	4.35	-8	58	14
L THA	47	0.78	4.07	-16	-10	4
L SFGmed	30	0.89	4.01	-8	40	42
L ANG, MOG	48	0.78	3.98	-48	-72	36
B ORBsupmed, ACG	101	0.45	3.96	-12	50	-6
			3.81	-2	54	-8
L MTG	48	0.78	3.91	-52	-24	-14
L SFGmed, DCG	38	0.84	3.85	-8	26	36
R HIP	16	0.96	3.64	22	-12	-14
Delayed > native (df = 37)						
L PHG	15	0.96	4.13	-20	-10	-32
Native signers (n = 16)						
L MTG, STG, TPOsup, ITG	442	0.004	7.45	-58	4	-18
			4.86	-50	-22	-14
L ORBinf, ORBmid	395	0.006	7.35	-30	32	-14
			5.45	-24	46	-18
L MTG, ANG, MOG, SMG, IPL, ITG, STG	2068	<0.001	6.95	-50	-52	22
			6.66	-48	-42	32
			6.33	-48	-72	36
L SFGdor, B SFGmed	730	<0.001	6.95	-10	52	34
			6.15	-10	58	26
			5.92	-12	60	18
L IFGtriang, MFG	492	0.003	5.72	-40	32	26
			5.08	-48	32	20
			5.03	-50	28	12
Delayed signers (n = 23)						
L PHG	54	0.72	5.76	-20	-8	-30
R ANG, IPL	145	0.22	5.72	40	-60	40
L MOG, SOG	195	0.11	5.18	-28	-72	34
			3.82	-38	-74	28
L IPL	186	0.13	4.94	-52	-40	48
			3.83	-42	-38	38
L TPOsup	25	0.92	4.84	-46	12	-24
R SFGdor	13	0.98	4.25	18	54	16
L ORBmid, ORBsup, ORBinf	37	0.85	4.25	-22	38	-12
L IFGtriang	52	0.74	4.18	-44	34	16
L MOG	24	0.93	4.16	-34	-90	18
L FFG, ITG	24	0.93	4.12	-38	-16	-30
L PoCG, IPL	12	0.98	3.93	-28	-42	48
L CAU	12	0.98	3.88	-6	10	-4
R ORBsup, ORBinf	21	0.94	3.85	24	32	-12
L ITG	26	0.92	3.79	-56	-52	-12
			3.78	-50	-50	-4

Notes: Clusters were reported at the threshold of voxel-level $p < .001$, cluster size > 10 voxels, except for the results of native signers, which were thresholded at voxel-level $p < .001$, cluster-level FWE-corrected $p < .05$. Two or three local maxima more than 8.0 mm apart were shown. L, left hemisphere; B, bilateral; R, right

bioRxiv preprint doi: https://doi.org/10.1101/2022.11.06.515336; this version posted November 7, 2022. The copyright holder for this preprint (which was not certified by peer review) is the author/funder, who has granted bioRxiv a license to display the preprint in perpetuity. It is made available under aCC-BY 4.0 International license.

hemisphere; ACG, anterior cingulate and paracingulate gyrus; ANG, angular gyrus; CAU, caudate; DCG, median cingulate and paracingulate gyrus; HIP, hippocampus; IFGtriang, inferior frontal gyrus, triangular part; IPL, inferior parietal lobule; ITG, inferior temporal gyrus; MFG, middle frontal gyrus; MOG, middle occipital gyrus; MTG, middle temporal gyrus; ORBinf, inferior frontal gyrus, orbital part; ORBmid, middle frontal gyrus, orbital part; ORBsupmed, superior frontal gyrus, medial orbital; PHG, parahippocampus; SFGdor, superior frontal gyrus, dorsolateral; PoCG, postcentral gyrus; SFGmed, superior frontal gyrus, medial orbital; SMG, supramarginal gyrus; SOG, superior occipital gyrus; STG, superior temporal gyrus; THA, thalamus; TPOsup, temporal pole: superior temporal gyrus.

bioRxiv preprint doi: https://doi.org/10.1101/2022.11.06.515336; this version posted November 7, 2022. The copyright holder for this preprint (which was not certified by peer review) is the author/funder, who has granted bioRxiv a license to display the preprint in perpetuity. It is made available under aCC-BY 4.0 International license.

Figure 3-Figure supplement 1

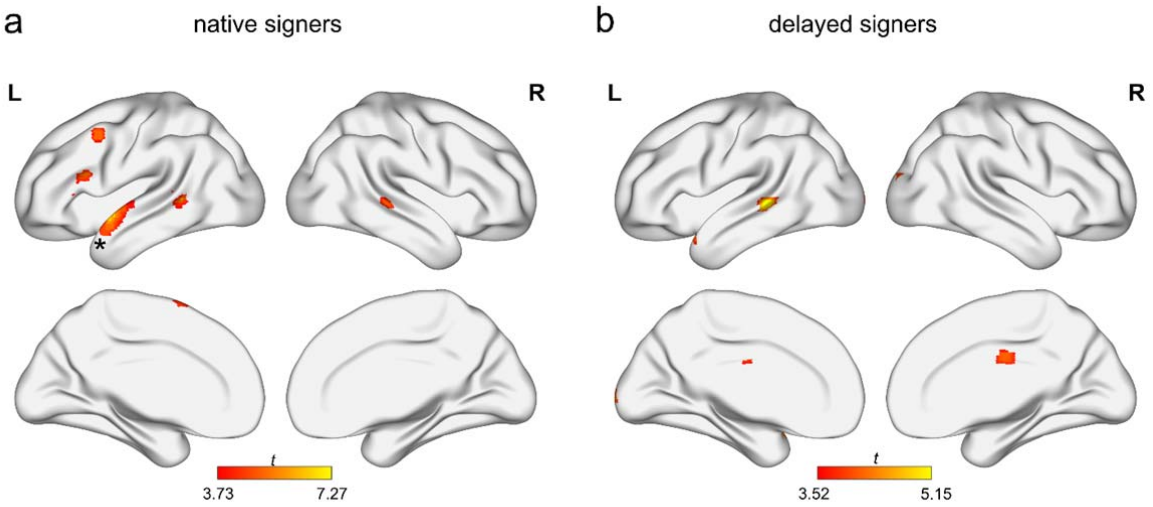

Whole-brain univariate contrast results of semantic abstractness in native (**a**) and delayed (**b**) signers. The neural effects were thresholded at voxel-level $p < .001$, cluster sizes > 10 voxels, and visualized using the "Maximum Voxel" mapping algorithm in BrainNet Viewer to illustrate small clusters. The asterisk in (a) indicates that the dATL cluster survived the cluster-level FWE-corrected $p < .05$. L, left hemisphere; R, right hemisphere. n = 16 in the native group; n = 23 in the delayed group.

bioRxiv preprint doi: https://doi.org/10.1101/2022.11.06.515336; this version posted November 7, 2022. The copyright holder for this preprint (which was not certified by peer review) is the author/funder, who has granted bioRxiv a license to display the preprint in perpetuity. It is made available under aCC-BY 4.0 International license.

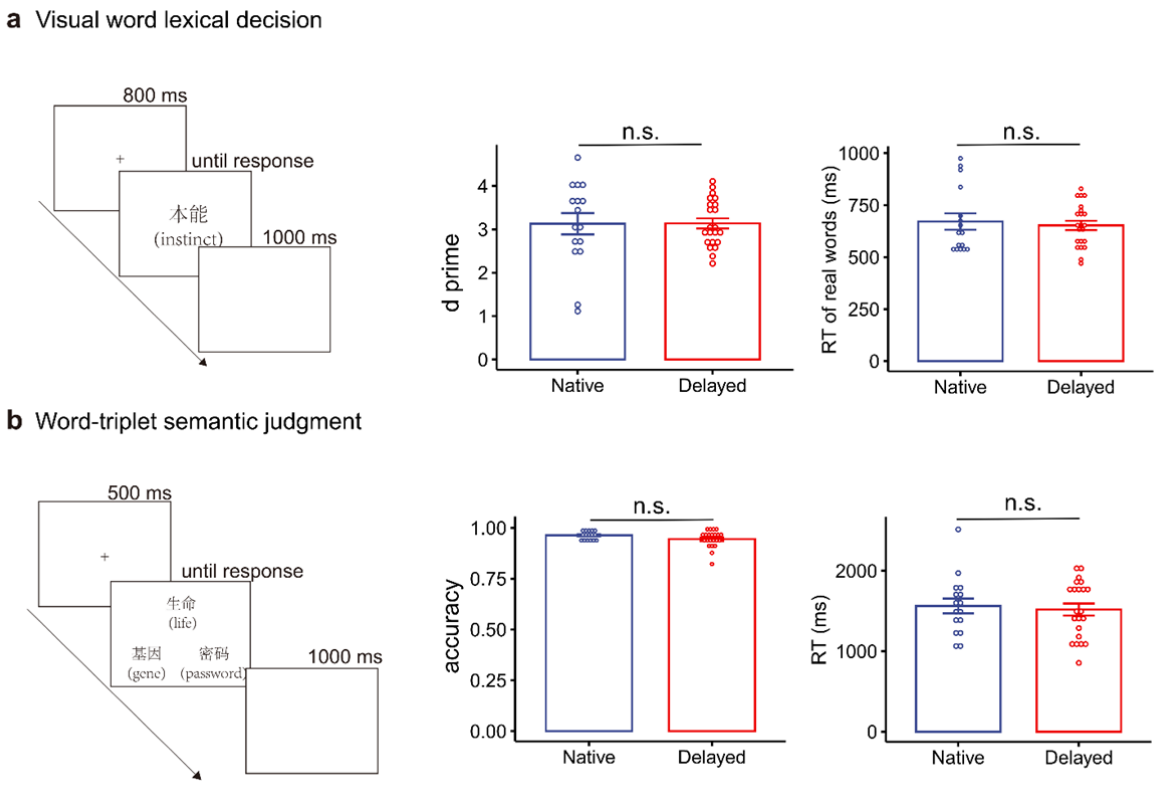

Native and delayed deaf signers did not significantly differ in written word processing in 2 behavioral reaction-time tasks. **a.** Lexical decision task, in which participants were asked to decide whether a 2-Chinese-character written stimulus denoted a real word or a pseudoword via button press. In each trial, a fixation point was presented for 800 ms, followed by a Chinese stimulus (font SONG, size 40). The stimulus disappeared upon the response and the next trial started 1 s later. The stimuli were 100 2-character Chinese nouns (word frequency, range: 0-1491 per million (Sun et al., 1997); number of strokes: range: 8-25) and 100 2-character pseudowords created by pseudo-randomly combining 2 characters of 100 real words. Bar plots show the d-prime and reaction time of real-word trials. d-prime was calculated using the Signal Detection Theory Calculator (version 1.2) provided by (Gaetano, 2017). **b.** Word-triplet semantic judgment task, in which participants were presented with three 2-character Chinese words and asked to decide which of the two choice words (bottom) was more semantically related to the probe word (top) via button press. In each trial, a fixation point was presented for 500 ms, followed by 3 Chinese words (font SONG, size 40), with the probe word presented at the top and two choice words arranged horizontally at the bottom. The stimuli disappeared upon the response and the next trial started 1 s later. The stimuli were 80 triplets of 2-character Chinese words (word frequency, range: 0 to 2340 per million; total number of strokes, range: 6-31), with all but four primarily used as nouns. Bar plots show overall accuracy and reaction time of correct trials. Both task procedures were implemented using E-prime 2 (Psychology Software Tools, Inc.; Pittsburgh, PA). n = 16 in the native group; n = 22 in the delayed group.

bioRxiv preprint doi: https://doi.org/10.1101/2022.11.06.515336; this version posted November 7, 2022. The copyright holder for this preprint (which was not certified by peer review) is the author/funder, who has granted bioRxiv a license to display the preprint in perpetuity. It is made available under aCC-BY 4.0 International license.

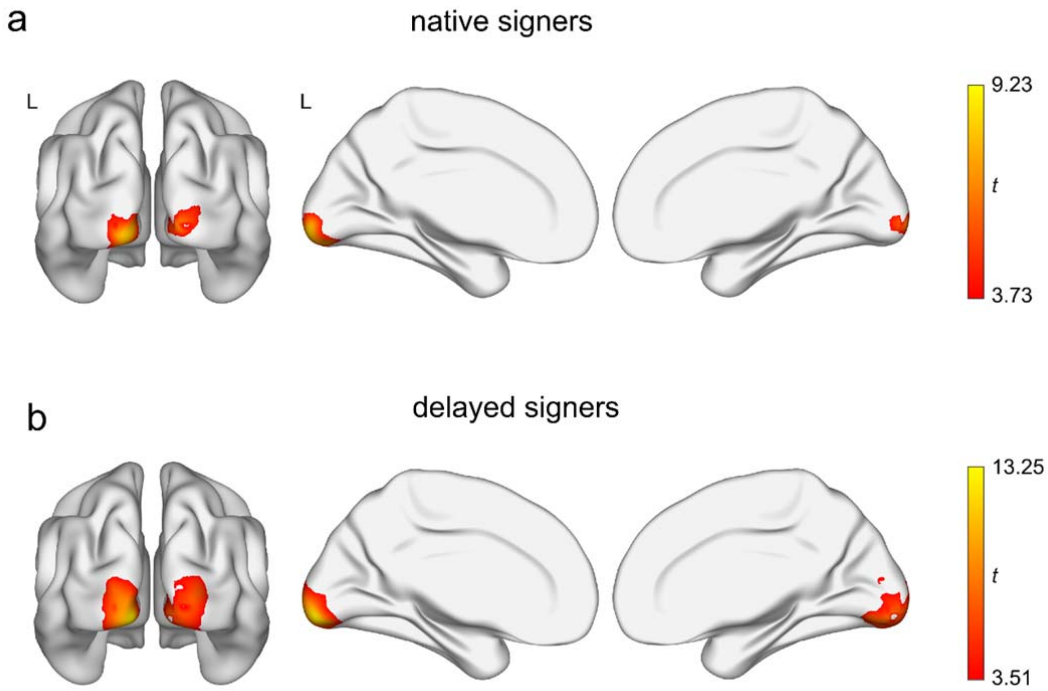

Whole-brain RSA results showed that pixelwise similarity of visual words were significantly encoded in early visual cortex in both native **(a)** and delayed **(b)** signers. The neural effects were thresholded at voxel-level $p < .001$, FWE-corrected $p < .05$. L, left hemisphere. n = 16 in the native group; n = 23 in the delayed group.